MASTERARBEIT | MASTER'S THESIS

Titel | Title

Tire-wear derived organic pollutants differentially impact the growth of representative human gut strains

verfasst von | submitted by

Aleksandra Stevanovic

angestrebter akademischer Grad | in partial fulfilment of the requirements for the degree of

Master of Science (MSc)

Wien | Vienna, 2026

Studienkennzahl lt. Studienblatt | Degree programme code as it appears on the student record sheet:	UA 066 830
Studienrichtung lt. Studienblatt | Degree programme as it appears on the student record sheet:	Masterstudium Molecular Microbiology, Microbial Ecology and Immunobiology
Betreut von | Supervisor:	Univ.-Prof. Dipl.-Biol. Dr. Alexander Loy

Acknowledgements

First, I would like to express my sincere gratitude to Prof. Alexander Loy for giving me the opportunity to carry out my master's thesis in his research group. The gut microbiome has been my first choice of research interest, and I am especially grateful to have been able to work on a topic I am truly passionate about within such a stimulating scientific environment.

I am especially thankful to my supervisor, Claire Lamb, for her continuous support, guidance, and encouragement throughout this project. Her insightful feedback, patience, and openness to discussion were invaluable at every stage of this work. I am particularly grateful for her willingness to share her expertise, help troubleshoot challenges, and encourage independent thinking, which greatly contributed to both the quality of this thesis and my development as a researcher. Her supportive and approachable mentorship made this experience both productive and enjoyable.

I would also like to thank all members of the Loy group for their support, engaging discussions, and constructive feedback during the group meetings. The collaborative atmosphere and exchange of ideas greatly enriched this experience.

My heartfelt thanks go to my boyfriend, Miroslav, for his constant support, understanding, and encouragement throughout this journey. His patience and positivity helped me navigate both the challenges and successes of this work.

Finally, I am deeply grateful to my family, especially my mom, for her unwavering support, encouragement, and belief in me. Without her, this would not have been possible.

Abstract

Tire wear particles (TWPs) are an abundant and emerging source of environmental pollution, representing a complex mixture of organic compounds, including benzothiazoles and diphenylguanidine (DPG), which have been increasingly detected across multiple environmental matrices as well as food products. Despite growing concern regarding human exposure, their impact on the gut microbiome remains poorly understood. The aim of this study was to investigate whether selected environmentally relevant TWPs-derived compounds, 2-mercaptobenzothiazole (MBT), 5-methyl-1H-benzotriazole (MHBT), and diphenylguanidine (DPG), impact the growth of representative human gut bacterial strains using high-throughput growth inhibition assays. In particular, this work sought to determine whether these compounds alter growth dynamics in pure cultures, which may suggest the potential to result in shifts in microbial composition and, thus ultimately, gut dysbiosis, as well as to explore the underlying mechanisms of any observed effects.

Across a wide concentration range (ng/L to mg/L), most strains exhibited substantial tolerance to both benzothiazoles and DPG, with no biologically relevant growth inhibition observed at environmentally relevant and higher concentrations. However, strain-specific responses were identified, with *Collinsella aerofaciens* displaying a consistent slight delay in the onset of exponential growth following exposure to MBT and MHBT, independent of their concentration. This effect was transient, with cultures fully recovering during prolonged incubation, indicating an impact on early growth kinetics as opposed to long-term viability. Notably, supplementation with trace minerals alleviated the observed delay in growth, suggesting metal chelating activity by benzothiazoles may contribute to the underlying mechanism.

Understanding how exposure of core gut microbiome strains to these xenobiotics influences their growth behavior provides insight into potential perturbations that may occur within the complex gut ecosystem. Such knowledge is essential for assessing possible downstream health consequences associated with environmental exposure to pollutants. Emerging evidence suggests that xenobiotics can induce functional changes, such as altered short-chain fatty acid production, independently of changes in microbial abundance. Therefore, while direct growth inhibition by TWPs-derived compounds may be minimal, potential impacts on microbial function, interspecies interactions, and long-term community dynamics cannot be excluded. Nonetheless, this study demonstrates overall substantial tolerance of selected gut strains to TWPs-dervied compound exposure, strain specific impacts on growth dynamics and offers initial mechanistic insights into the modes of action of these compounds. This work thus establishes a foundation for future research, which could be applied to complex microbial communities to better understand the implications for gut microbiome stability and host health.

Table of Contents

Introduction

Contaminants emitted from consumer products represent a major source of environmental pollution in Western countries (Wik A., 2009; Roux I., 2025). In the case of tire wear particles (TWPs), increasing concern has emerged due to both their widespread presence and the demonstrated toxicity of certain derivatives, particularly 6PPD-quinone (6PPD-Q) in aquatic systems (Ghanadi M., 2025). Notably, over one million tons of TWPs are generated annually within the European Union alone (Wagner S., 2018). Despite this substantial input, research has primarily focused on airborne tire-derived compounds, whereas the toxicity of non-exhaust TWPs-derived compounds remains poorly understood, despite these accounting for an estimated 90–99.9% of TWPs in the environment (Wagner S., 2018).

Recent studies have demonstrated that TWPs-derived compounds, including benzothiazoles, diphenylguanidine (DPG), and phenylenediamines, can accumulate in commercially available leafy vegetables, thereby providing a route of exposure to the human gut microbiome (Castan, et al., 2022; Sherman, 2024). In one study, maximum concentrations detected in leafy vegetables reached 2.29 µg/g for DPG and 1.24 µg/g for benzothiazole (Castan, et al., 2022). In a separate study, maximum concentrations reported on a dry weight basis were 238 ng/g dw for benzothiazole, 665 ng/g dw for 2-hydroxybenzothiazole, and 2.1 ng/g dw for DPG (Sherman, 2024). Drinking water is another potential human exposure route for TWPs-derived chemicals relevant to the gut microbiome. A recent study detected nine tire-related compounds in drinking water sources and treatment plant samples, and estimated human daily intake via drinking water at 2.63×10^{-8} to 3.16×10^{-5} mg/kg body weight/day, indicating chronic low-level exposure (Zhang H. Y., 2023). Further, benzothiazoles may also represent a dietary exposure route through seafood consumption. In a study conducted in Spain, benzothiazoles were detected in ten 7ommercially available seafood species, including mussel, squid, shrimp, salmon, and sardine (Trabalón, 2017). The highest total concentrations were observed in squid (82 ng/g dry weight), while benzothiazole was detected in nearly all tested samples, indicating that seafood may contribute to chronic low-level human exposure to these contaminants (Trabalón, 2017). This is particularly relevant given the essential roles of the gut microbiome in host health. The human gut microbiome is a complex and dynamic community of trillions of microorganisms, including bacteria, fungi, and archaea, that inhabit the gastrointestinal tract (Sekirov, 2010; Santoro, 2018). The microbiota plays a key role in maintaining host health including contributing to immune system regulation, protection against pathogen colonization, support of epithelial cell function, and enabling the digestion of otherwise indigestible complex carbohydrates (Gomaa, 2020; Jovel, 2018). In addition, it is involved in vitamin synthesis and metabolic regulation, as well as through the gut–brain axis, influencing neurological and mental health (Gomaa, 2020; Jovel, 2018). This ecosystem is shaped by multiple host and environmental factors, with the latter including diet, lifestyle, antibiotic exposure, and environmental pollutants, resulting in high inter-individual variability (Santoro, 2018). A healthy microbiome is characterized by diversity, stability, and resilience, and includes both abundant taxa as *Akkermansia muciniphila*, and functionally important low-abundance keystone taxa such as *Bacteroides caccae,* and *Collinsella* spp., with presence being essential for maintaining community structure and function (Lozupone, 2012; Trosvik, 2015; Tudela, 2021).

Exposure to xenobiotics, i.e. synthetic compounds originating from environmental pollution, food, and industrial processes, is an unavoidable aspect of modern life, with the gastrointestinal tract serving as a major entry point for human exposure (Tsiaoussis, 2019;

Štefanac, 2021). In addition to ingestion, xenobiotics may also enter the body through inhalation of airborne particles and vapors, dermal absorption following contact with contaminated surfaces or products, and in some cases prenatal transfer, thereby contributing to the overall human exposure burden (Wu, 2025). Ingested compounds may be metabolized by the gut microbiome, influencing their bioavailability and toxicity, but also have the potential to disrupt microbial homeostasis, leading to dysbiosis (Croom, 2012; Chi, 2021). Dysbiosis, defined as an imbalance in microbial composition or function, has been linked to numerous diseases, including inflammatory bowel disease, metabolic disorders, and neurological conditions via the gut–brain axis (Bidell, 2022; Perez, 2020; Das, 2019; Lozupone, 2012; Carding, 2015). Further, there is increasing evidence which indicates that environmental pollutants, including pesticides and persistent organic pollutants, can alter gut microbial composition and thereby their function, even after short-term exposure (ranging from 24h to 4 weeks dependant on class of pollutant) (Castañeda-Monsalve, 2024; Jin Y. W., 2017; Lefever, 2016; Roux I., 2025). Similarly, large-scale screening studies have shown that many anthropogenic chemicals exert strain-specific inhibitory effects on gut bacteria, highlighting the sensitivity of the microbiome to chemical exposure and the potential for environmental contaminants to influence host–microbiome interactions (Roux I., 2025). Therefore, investigating the impact of these compounds on key members of the gut microbiota is essential to better understand their potential role in microbiome perturbation and thus associated health outcomes.

Tire Wear Particles are Highly Complex

TWPs are compounds commonly found in the tires of various commercial and consumer vehicles (Johannessen C. L., 2022). These particles account for 5-30% of non-exhaust emissions from the traffic, with approximately 1,327,000 t annually generated in European Union solely (Wagner S., 2018). In Germany 133,000 tons of TWPs are estimated to be released annually, exceeding the country's total pesticide utilization by more than four times (Wagner S., 2018). While the total non-exhaust particulate emissions generated by traffic are widely acknowledged as potentially harmful to the environment, data specifically addressing TWPs remains limited (Wagner S., 2018).

Most modern tires are made from synthetic material, derived from petroleum (Johannessen C. L., 2022). As a result, the main component of the modern passenger tire is rubber, either natural or synthetic such as butadiene rubber or styrene butadiene rubber, accounting for 40-50% of the tire composition (Figure 1) (Sommer, 2018). This is followed by 30-35% of filters, such as carbon black, and softeners, such as resin or oil (Sommer, 2018). The remaining composition includes 5-10% of additives, including hexamethoxymethylmelamine (HMMM), a linking agent, and 2-5% vulcanization agents (Johannessen C. L., 2022; Sommer, 2018). During the vulcanization process, different compounds such as sulfur, benzothiazoles and N,N′-diphenylguanidine (DPG) are added to enhance elasticity and accelerate transformation during the process, respectively (Wagner S., 2018; Tumwet, 2025; Alotaibi, 2015; Tkalec, 2023). Consequently, TWPs are highly complex particles, composed of rubber polymers, various organic compounds, metals (usually zinc – Zn and sulfur – S) and road-derived materials, which can contribute to environmental pollution (Wagner S., 2018; Tumwet, 2025).

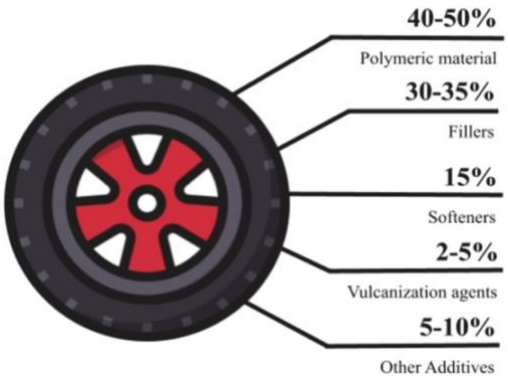

Figure 1: Standard passenger car tires are chemically complex, **with polymers such as rubber accounting for the majority of the composition.** Figure from Sommer, 2018.

Tire Wear Particles are Environmentally Widespread

The environmental fate of TWPs) is strongly influenced by their physical properties, particularly particle size (Wagner S., 2018). TWPs can be broadly classified by size into coarse (PM_{10}, 2.5–10 µm), fine ($PM_{2.5}$, 0.1–2.5 µm), and ultrafine ($PM_{0.1}$, <0.1 µm) particles (Wagner S., 2018). Additionally, TWPs can be classified as airborne or non-airborne (Wagner S., 2018). Airborne TWPs form when heat from tire-road friction causes volatile compounds to evaporate and condense into microparticles (Mathissen, 2011). Despite being comparatively more well-studied, airborne TWPs represent only 0.1–10% of total emissions, therefore 90–99.9% are non-airborne (Wagner S., 2018). Given this, it is clear that further work is required to assess the impacts of the majority of these key contributors to non-exhaust emissions in the environment and beyond (Wagner S., 2018).

The concentration of TWPs is typically highest on the roadsides and can differ between different areas as transport pathways and the generation itself is dependant on factors such as drainage systems and the type of road (Kundel, 2025; Baensch-Baltruschat, 2021). Few studies have quantified TWPs levels in roadside soils. Müller at al. (2022) reported concentration ranging from 155 to 15,898 mg/kg in Germany, while Kundel et al. (2025) found average counts of 111,000 TWPs/kg soil, with peaks up to 615,000 TWPs/kg and a mean TWPs mass of 52.7 ± 83.2 mg/kg. TWPs typically accumulate in the top layer of the soil (Tumwet, 2025) but the fate of these particles is influced by factors such as weather conditions and urban infrastructure further influencing the transportation and distribution of these TWPs (Wagner S., 2018). Additionally, these particles have been demonstrated to penetrate from the roads to wastewater treatment plants, rivers, and other water bodies (Figure 2) (Wagner S., 2018). This movement therefore leads to the contamination of surface waters and the pedosphere as well as agricultural soils, thus providing a key entry route into the human food chain (Wagner S., 2018; Baensch-Baltruschat, 2021).

Within all environmental compartments, soil, water, and air, pollutants released from tire wear particles can undergo chemical transformations, with the potential to result in the formation of more toxic and biologically potent compounds (Johannessen C. L., 2022). Specifically, antioxidant N-(1,3-dimethylbutyl)-N′-phenyl-p-phenylenediamine (6PPD) is of particular recent interest environmentally as it has been shown to transform into 6PPD-quinone (6PPD-Q) in aquatic environments (Johannessen C. L., 2022). This transformation product has

been identified as toxic to aquatic organisms, as evidenced by its lethality to coho salmon (*Oncorhynchus kisutch*) in exposure studies, with the Lethal Concentration 50 (LC50) being only 0.79 ± 0.16 ng/L (Tian, 2021).

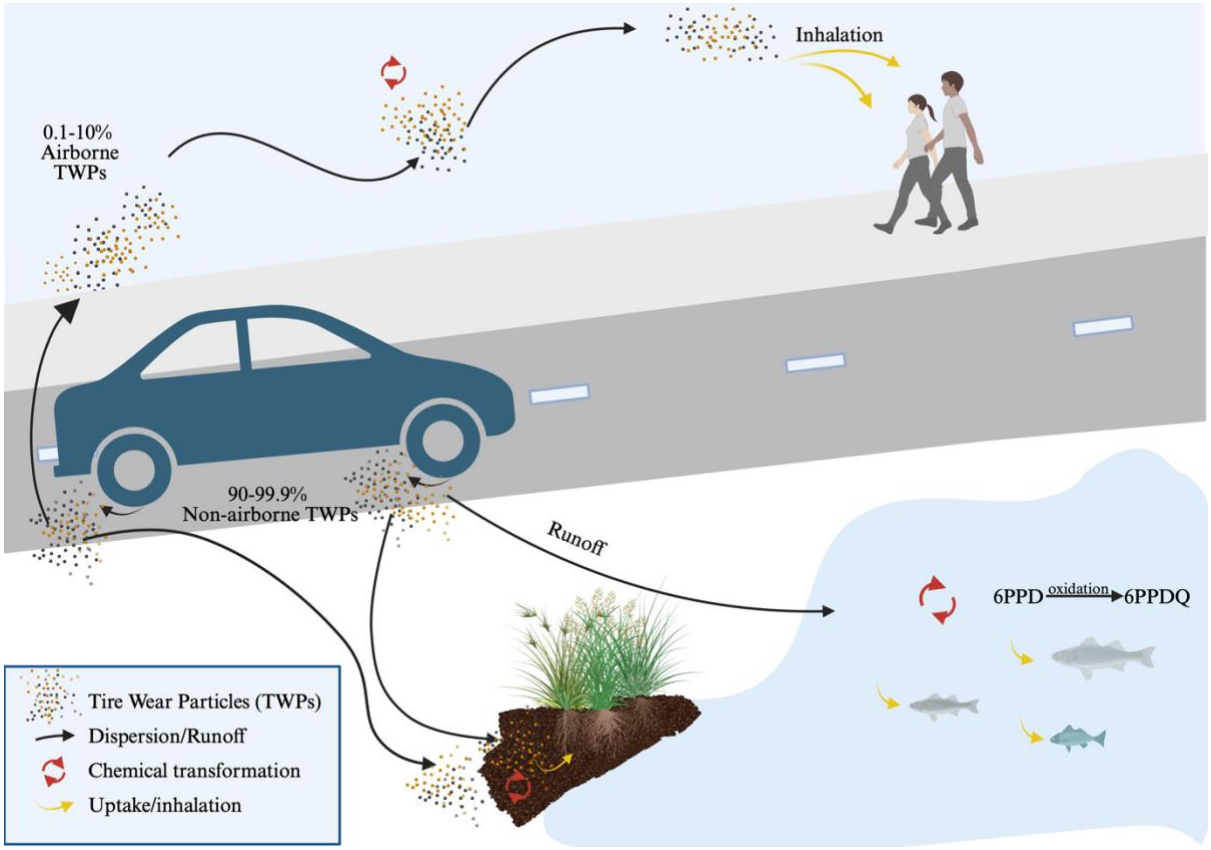

Figure 2: Tire wear particles are widely distributed across environmental compartments including air, soil, and water. TWPs are primarily generated and accumulate along road surfaces, from where they are dispersed into surrounding environments, where they can be transferred to soil and transported to aquatic systems via runoff. In all compartments (air, soil, and water) TWPs and the leached compounds undergo chemical transformation processes, including photochemical, hydrolytic, and microbial reactions and oxidation (e.g. oxidation of 6PPD to 6PPD-Q in aquatic environment), generating secondary products with altered mobility and toxicity (Zeb, 2026). TWPs and leached compounds can further be taken up by plants from contaminated soil and ingested by fish and other aquatic organisms within the receiving water body. Human exposure may occur through inhalation, ingestion from both contaminated plants and food (fish, sea food etc) while their persistence is driven by continuous transformation and redistribution across environmental systems. Arrows indicate different processes: yellow for inhalation/uptake, red for chemical transformation, and black for transport between different environments (e.g., water, soil, etc.). Figure created in Biorender (https://BioRender.com).

Tire Wear Derived Compounds are Toxic to a Range of Organisms

Tire wear particles (TWPs) have various effects on aquatic organisms such as zebra fish (*Danio rerio*), including growth retardation, gene dysregulation, gut microbiome disruption, and oxidative stress, with smaller particles inducing more severe responses (Song, 2025). However, this study assessed the effects of tire wear particles as complex mixtures

rather than individual compounds (Song, 2025). Although this approach is environmentally relevant, it makes it difficult to attribute the observed biological effects to specific chemical constituent. Multiple studies have demonstrated both TWPs and their leachates can impair mobility, reproduction, and survival in species such as copepods (*Daphnia magna*) with contaminants such as zinc and pyrene from the leachate playing key toxic roles (Liu J. F., 2023) and the majority of studies assessing impact of TWPs focusing on inorganic additives. However, organic TWPs-derived compounds such as 6PPD and 6PPD-Q have been shown to induce oxidative stress and metabolic disruptions in the algae *Chlorella vulgaris*, these impacts result from a compromise in cell membrane integrity, with 6PPD-Q exerting comparatively more pronounced effects (Liu J. Y., 2024).

Additionally, tire wear particles have been observed to negatively affect soil organisms such as worm *Enchytraeus crypticus* by reducing survival, reproduction and altering the gut microbial communities of the worm (Ding, 2020). Moreover, TWPs-derived compounds like benzothiazoles, particularly benzothiazole (BTZ) and 2-hydroxybenzothiazole (HBT), the dominant BTZs detected in soils, are found to be detrimental to fungal biomass and thus could disrupt soil fungal community structure (Peng, 2024). In this study effects induced with complex TWPs and pure compounds were investigated in soil samples, confirming that these impacts were primarily driven by benzothiazoles, particularly 2-hydroxybenzothiazole (HBT), indicating that TWPs toxicity is largely mediated by associated chemical additives rather than the particles themselves (Peng, 2024). This data was further validated with pure culture experiments with two representative species of fungi, *Eurotium cristatum* and *Polyporales ostreatus* (Peng, 2024). These studies underscore the potential for broad ecological risks posed by these pollutants demonstrated in both aquatic and terrestrial environments, which remains poorly understood in other systems.

Benzothiazoles are aromatic chemical compounds widely used with various applications (Alotaibi, 2015; Tkalec, 2023) including in industrial fluids, photographic processes and leather treatment among other applications (Tkalec, 2023). Benzothiazole derivatives such as 2-mercaptobenzothiazole (MBT) and 5-methyl-1H-benzotriazole (MHBT) (Figure 3) are commonly employed as vulcanization accelerators in tire manufacturing, specifically in the volcatization process as accelerators (Alotaibi, 2015; Tkalec, 2023). Additionally, MBT is well known for its affinity for metal ions, with the ability to chelate various metals, including copper (Cu), cobalt (Co), zinc (Zn), and lead (Pb), as well as metal sulfide and precious metal ores, through coordination via its sulfur (S) and nitrogen (N) atoms (Figure 4) (Yekeler, 2006).

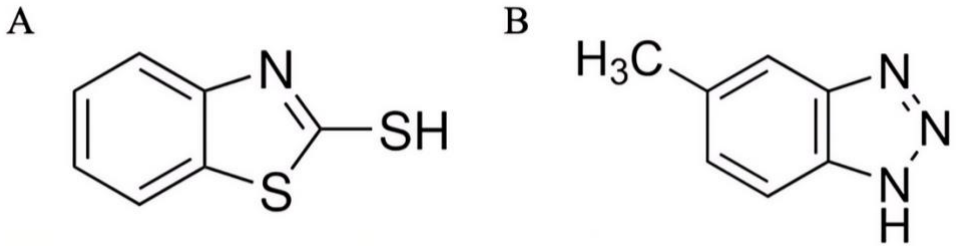

Figure 3: Chemical structures of 2-mercaptobenzothiazole (MBT, A) and 5-methyl-1H-benzotriazole (MHBT, B). Images sourced from Sigma-Aldrich (https://www.sigmaaldrich.com).

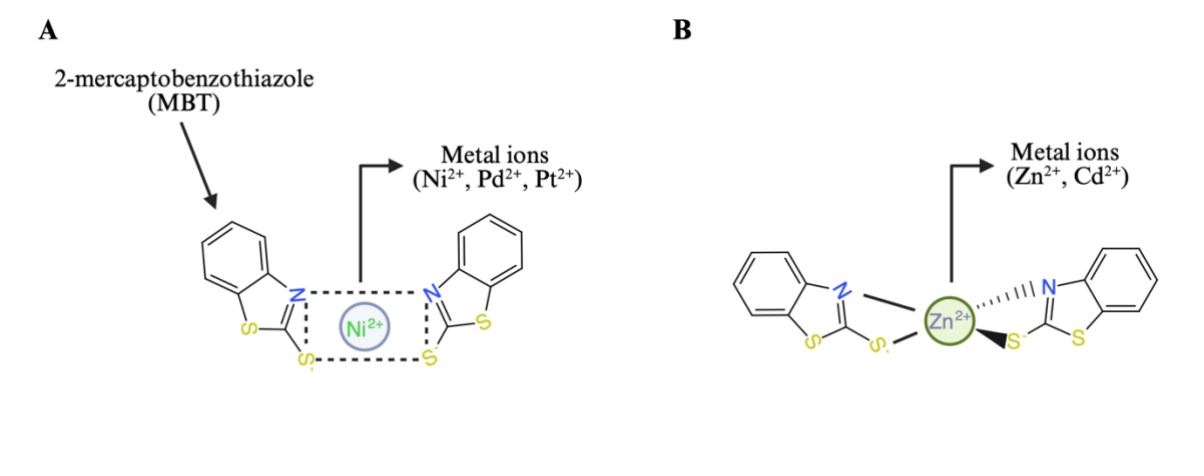

Figure 4. 2-Mercaptobenzothiazole (MBT) is known to form coordination complexes with various metal ions through chelation via the thiazole nitrogen (N) and exocyclic sulfur (S) donor atoms. (A) With nickel(II) (Ni^{2+}), palladium(II) (Pd^{2+}) and platinum(II) (Pt^{2+}), MBT forms bis-ligand complexes with a cis square-planar geometry, proposed from infrared spectroscopy, magnetic measurements and electronic spectra. (B) With zink(II) (Zn^{2+}) and cadmium(II) (Cd^{2+}), MBT forms bis-ligand complexes with probable tetrahedral geometry through the same N,S-bidentate binding mode. Based on Banerji, 1982. Figure created in Biorender (https://BioRender.com)

Benzothiazoles are highly stable in aquatic environments due to their low volatility, and therefore can persist for extended periods (Alotaibi, 2015). They are also resistant to oxidation, and their biodegradation proceeds slowly (Alotaibi, 2015). These compounds are suspected to be carcinogenic and genotoxic, and also suggested to adversely affect the respiratory tract and disrupt the endocrine system (Liao, 2018). Environmental monitoring indicates that benzothiazoles may occur at levels up to 2,500 µg/L in surface water, 49.3 µg/L in wastewater, 50.2 µg/kg in sludge, and 32 µg/m³ in atmospheric sample (Liao, 2018). This detection, stability and wide usage making them of particular of environmental, and thus human health, concern.

High production-volume chemical 1,3-Diphenylguanidine (DPG) (Figure 5) is widely used as a catalyst in tire manufacturing, where it accelerates sulfur cross-linking during rubber vulcanization (Johannessen C. H., 2022). DPG has also been detected in household devices such as tap-water aerators, electronic equipment, flooring, building materials and furniture, as well as in childrens toys, indicating notable potential for domestic exposure (Johannessen C. H., 2022; Li Z. M., 2023). Environmental monitoring has revealed varying presences of DPG in various matrices, including surface waters in Toronto at concentrations up to 0.52 µg/L, in drinking-water supplies in Singapore at 0.25–32.6 ng/L, air across 18 different cities, indoor air (where it occurs as phenylguanidine) at approximately 0.339 pg/m³, household dust from 11 different countries at levels around 140 ng/g and soil samples from northeastern United States at median concentration of 380 ng/g (Johannessen C. H., 2022; Johannessen C. S., 2022;

Li Z. M., 2023; Li Z. M., 2023; Marques dos Santos, 2023). Toxicological studies have demonstrated developmental toxicity in aquatic models, such as fathead minnow (*Pimephales promelas)* embryos, while *in vitro* high-throughput screening assays have suggested potential neurotoxic and endocrine-disrupting effects (Li Z. M., 2023; Shin H. M., 2020). In humans, exposure to DPG has been associated with allergic contact dermatitis, and its presence has been detected in biological samples, including maternal and cord serum (Li Z. M., 2023), underscoring the need for further evaluation of its environmental and human-health impacts. Despite these findings, the effects of DPG on human systems, including the gut microbiome, remain largely unexplored, representing an important gap in understanding its potential impact on host–microbiome interactions.

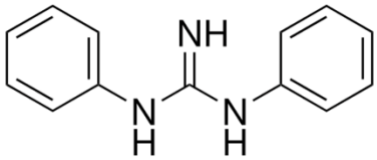

Figure 5: Chemical structure of 1,3-diphenylguanidine (DPG). Images sourced from Sigma-Aldrich (https://www.sigmaaldrich.com).

Occurrence of Tire-Wear Particles and Associated Chemicals in Commerically Available Food Products and Drinking Water

In addition to the aforementioned harmful ecological impacts, TWPs may pose a risk to food safety. It was demonstrated in a study that TWPs-derived compounds (including DPG, HMMM, BTZ, 6PPD, and 6PPD-Q) are readily taken up by lettuce and translocated to edible leaves (Castan, et al., 2022). Additionally, this study demonstrated the formation of that several stable transformation in plants, which often persisted longer than the associated parent compound (Castan, et al., 2022). HMMM showed the highest accumulation of 20 µg/g, while DPG conjugates and BTZ oxidation products also proved to be stable, however with around 2-3 times lower accumulation potentiation comparing to HMMM (Castan, et al., 2022).

Further, a recent study confirmed the accumulation of TWPs-derived compounds in commercially available leafy vegetables detecting six such chemicals across samples originating from multiple countries, including Switzerland, Italy, Israel and Spain (Sherman, 2024). Benzothiazole and 2-hydroxybenzothiazole demonstrated the highest concentrations at 238 and 665 ng/g dry weight, respectively, whilst other compounds like 6PPD, N-Isopropyl-N-phenyl-4-phenylenediamine (IPPD), and DPG were present at significantly lower levels (Sherman, 2024). Notably, at least one of these compounds was found in 71% of the samples analyzed. This study estimates daily intake values, identifying benzothiazole as the compound with the highest potential exposure, ranging from 12-1,296 ng/person/day (Sherman, 2024).

Another study conducted in Spain (Catalonia) reported the accumulation of benzothiazoles in commercially available seafood products (Trabalón, 2017). Benzothiazoles were investigated in ten seafood species, including mussels, squid, shrimp, salmon, and sardines (Trabalón, 2017). Benzothiazole was detected in nine out of ten sample, with the highest detected concentration of in squid (82 ng/g dry weight), following by mussels (58 ng/g

dry weight) (Trabalón, 2017). Mussels were the only species in which all five analyzed benzothiazole compounds were detected, while squid, sardines and hike contained four out of five contaminants (Trabalón, 2017). These findings indicate that seafood products may represent an important route of chronic low-level human exposure to benzothiazoles and highlight the potential for bioaccumulation of these contaminants within aquatic food webs.

Additionally, TWPs have also detected in drinking water in China, representing a potential route for human exposure to TWPs-derived chemicals relevant to the gut microbiome (Zhang H. Y., 2023). In a recent study, nine tire-related compounds were identified in drinking water sources and treatment plant samples, with estimated human daily intake via drinking water at 2.63×10^{-8} to 3.16×10^{-5} mg/kg body weight/day indicating chronic low-level exposure (Zhang H. Y., 2023).

The Human Gut Microbiome is Vital for Host Health

The gut microbiome refers to the community of microorganisms, including bacteria, fungi, and archaea, that inhabit our gastrointestinal tract (Sekirov, 2010). It is estimated that trillions of microbes reside in the human gut (Santoro, 2018), with the colon being the most densely populated, containing about 10^{11} microbes (Sekirov, 2010).

This dynamic ecosystem plays vital roles in maintaining health, developing the immune system, regulating physiological processes, and influencing disease onset (Jin Y. C., 2023; Santoro, 2018). Furthermore, the gut microbiome interacts with various host organs through the "gut-organ axis" (Jin Y. C., 2023). Multiple factors are known to affect the compositon of the gut microbiome's, including diet, gender, age, lifestyle, ethnicity, mode of birth (C-section or vaginal delivery), type of infant feeding (breastfeeding or formula), antibiotic use during early development, and environmental factors such as pollution exposure and use of pharmaceuticals (Santoro, 2018). All of these factors shape the microbiome and contribute to inter-individual variability in gut microbiome composition.

A healthy gut microbiome can be described by its diversity, resilience, dynamics, richness, and stability (Lozupone, 2012). It is predominantly composed of key bacterial phyla such as *Firmicutes*, *Proteobacteria*, *Bacteroidetes*, and *Actinobacteria*, alongside less-represented groups like *Tenericutes*, *Fusobacteria*, *Verrucomicrobia*, and *Spirochetes* (Das, 2019). Microbiome composition is highly diverse, with hundreds of bacterial species influenced by host signals and environmental factors (Santoro, 2018; Zhu, 2010). In addition to highly abundant gut species known as 'foundation' species such as *Akkermansia muciniphila* and *Bacteroides thetaiotaomicron*, the gut microbiome also contains keystone taxa, low-abundance species such as *Collinsella* spp., *Bacteroides caccae* and *Bacteroides fragilis* with the loss of these species having a potentially profound impact on community structure and function due to their involvement in key metabolic processes (Tudela, 2021; Trosvik, 2015; Shin J. H., 2024).

Xenobiotics Interact with the Gut Microbiome in Multiple Ways

Due to anthropogenic activities many compounds that interact with the gut microbiome, particularly through ingestion, are not naturally occurring and cannot be biosynthesized

(Štefanac, 2021; Rieger, 2002). These are known as xenobiotics, defined specifically as synthetic chemicals which are either entirely unnatural or distinct from natural compounds in structure or stereochemistry (Štefanac, 2021; Rieger, 2002). They often contain features that biological systems are unable to produce, such as multiple methyl groups on aliphatic or aromatic rings, which makes them difficult for microorganisms to metabolize (Rieger, 2002). Xenobiotic compounds are found in drugs, pollutants, food additives, and industrial chemicals (Figure 6) (Jin Y. C., 2023) and human exposure to these compounds is often unavoidable, entering the body through routes such as ingestion (Tsiaoussis, 2019).

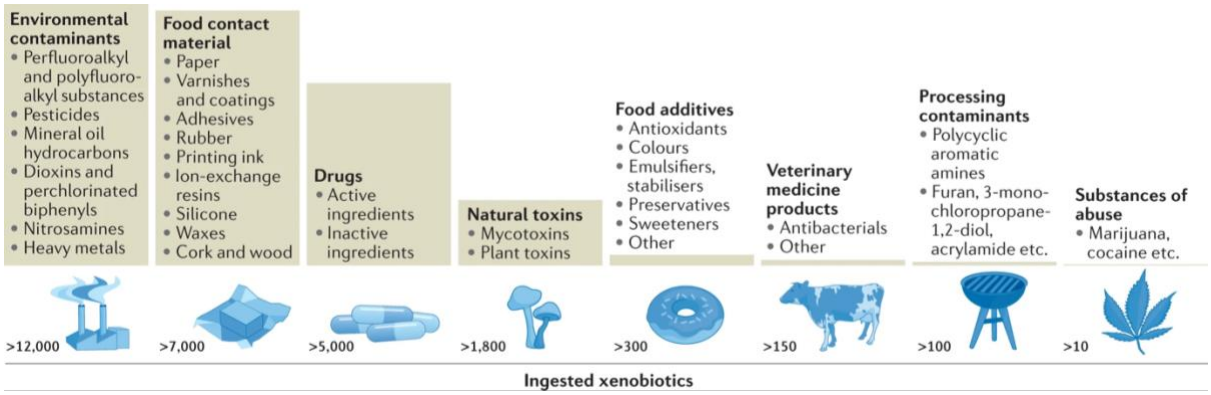

Figure 6: Xenobiotics compounds entering the human gastrointestinal tract (GI) come from multiple primary sources including environmental contaminants, food contact materials, pharmaceuticals, natural toxins, food additives, veterinary drugs, processing contaminants, and substances of abuse. Environmental contaminants represent the largest group (>12,000 compounds), followed by food contact materials (>7,000) and drugs (>5,000). These diverse compounds are introduced mainly through ingestion and contribute to the continuous exposure of the gut microbiome to a wide range of chemically distinct substances. Figure from Lindell A. E.-K., 2022.

The gastrointestinal tract serves as a major entry point for xenobiotics where these compounds can alter key microbial metabolites such as bile acids, short chain fatty acids (SCFAs), branched-chain amino acids, tryptophan derivatives and trimethylamine N-oxide (Jin Y. C., 2023). Through the circulation, molecules produced by gut microbial strains can directly influence the biological functions of host organs through immune, hormonal, metabolic, neural, and endocrine signaling pathways (Jin Y. C., 2023). This bidirectional communication network is referred to as gut-organ axis, allowing these gut-derived effects to extend to distant tissues and organ systems including gut-liver axes, gut-kidney axes, and other related pathways (Jin Y. C., 2023). Many xenobiotics are metabolized in the gut often reducing their toxicity and facilitating excretion, a process largely shaped by the gut microbiome which regulates their absorption, transformation, and systemic impact (Croom, 2012; Nakov, 2020). Exposure to certain xenobiotics disrupts microbial homeostasis, leading to dysbiosis (Chi, 2021).

Dysbiosis of the Human Gut Microbiome is Linked to Adverse Health Outcomes

Dysbiosis is an imbalance or disruption in the composition or function of the gut microbiome which deviates from a healthy state, therefore potentially impairing the ability to support host health (Bidell, 2022; Perez, 2020; Das, 2019). What is considered by the term "dysbiosis" is context and subject dependent and can be triggered by both environmental factors (e.g. lifestyle, diet, exposure to xenobiotics) and host-related factors as (e.g. genetics, host physiology) (Das, 2019). Several factors can disrupt microbial homeostasis and lead to dysbiosis, including the reduction or loss of keystone taxa, decreased alpha diversity (number and abundance of species), impaired metabolic functions, and the overgrowth of pathobionts (Das, 2019). Dysbiosis is generally classified into two categories: taxonomic dysbiosis, which involves changes in microbial composition, such as altered species abundance, reduced diversity, or the loss of keystone taxa, occurring at various taxonomic levels; and functional dysbiosis, characterized by shifts in microbial gene functions and metabolic profiles, even in the absence of consistent taxonomic changes, with both distinguishing patients from healthy individuals (Das, 2019).

Multiple studies have demonstrated associations between gut microbiome dysbiosis and a range of human diseases, including inflammatory bowel disease, type 2 diabetes, metabolic disorders, obesity, and colorectal cancer (Lozupone, 2012). Dysbiosis has also been implicated in altered cognitive function and behavior through the gut–brain axis, potentially contributing to neurological and psychiatric conditions such as Alzheimer's disease, Parkinson's disease, anxiety, and depression (Carding, 2015). A growing body of evidence indicates that environmental pollutants can disrupt gut microbial communities, impairing metabolism, nutrient absorption, immune function, and overall host health (Jin Y. W., 2017). Heavy metals, including arsenic, cadmium, and lead, have been shown to alter gut microbiota composition, which is linked to inflammation and metabolic disturbances in animal models (Zhang S. J., 2015; Lu, 2014; Lukovac, 2014). Exposure to these metals is further associated with carcinogenesis, immune dysfunction, diabetes, cardiovascular disease, and weight gain (Jin Y. W., 2017). Likewise, persistent organic pollutants (POPs) such as polychlorinated biphenyls PCBs, polycyclic aromatic hydrocarbons (PAHs), and dioxins have been shown to rapidly shift microbial community structure, frequently disrupting the gut microbiome composition, altering bile acid metabolism and metabolic function, and inducing gut and lung inflammation (Zhang L. N., 2015; Lefever, 2016; Jeong, 2025). These pollutant-induced microbiome changes, observed even after short-term exposure in animal models (after only 5 days and 1 week exposure to POPs and PAHs, in 8-week-old male C57BL/6J mice and eight-week-old female C57BL/6 mice, respectively) have been linked to inflammatory immune responses, metabolic disorders, and enhanced bioactivation of toxic compounds within the gut (Zhang L. N., 2015; Jeong, 2025; Van de Wiele, 2005).

Impacts associated with keystone gut strains can be useful to infer for the potential for more widespread dysbiotic potential. Consistent with aforementioned findings, a recent study by Roux et al. (2025) evaluated the effects of 1076 industrial chemicals, comprised of insecticides, herbicides, pesticides, fungicides, and related compounds, on 22 commensal gut bacterial strains. Screening revealed that only 168 of the tested substances inhibited the growth of at least one microbial strain, with members of the order *Bacteroidales* being particularly susceptible across chemical groups. Fungicides, acaricides and industrial chemicals exhibited the strongest overall impact, with ~30% demonstrating measurable growth inhibition activity on strains, while to other groups including herbicides, insecticides and PAHs, representative gut strains showed mostly tolerance at 20 μM concentration, with selected chemicals exhibiting inhibitory effects at concentrations as low as 2.5 μM, within the range of environmentally relevant exposures. These findings underscore the seemingly phylogenetic-specific

sensitivities of selected strains of the gut microbiota to a broad spectrum of anthropogenic chemicals, highlighting the potential for widespread environmental contaminants to influence host-microbiome interactions.

Aims and Objectives

The occurrence, accumulation, and toxicity of TWPs-derived compounds across environmental systems, as well as their detection in edible plants, raise important concerns regarding human exposure, particularly through the gastrointestinal tract and thus the associated microbiome. Given the critical role of the gut microbiome in maintaining host health and its previously well established, albeit often species-specific, sensitivity to certain xenobiotic exposures, our study aims to investigate how selected representative TWPs-derived compounds and their associated environmentally relevant transformation products, impact the growth of key representative strains associated with the healthy human gut microbiome. This thesis specifically seeks to address the following research objectives:

1) To assess the impact of selected environmentally relevant TWPs-derived compounds (MBT, MHBT, and DPG) on gut bacterial growth using high-throughput growth inhibition assays across environmentally relevant concentration ranges.

2) To determine the concentrations at which each selected TWP-derived compound induces measurable growth inhibition effects in pure cultures of representative gut bacterial strains.

3) To determine the presence of strain-specific sensitivity, characterize potential alterations in growth dynamics of the representative gut strains and resulting dysbiosis implications

4) To investigate the underlying mechanisms of observed effects and explore potential strategies to mitigate their impact on gut bacterial growth.

To investigate this a range of concentrations, both environmentally relevant and elevated, were incubated with ten representative human gut strains in pure culture, resulting in a high throughput screening for potential activity related to biological toxicity using growth dynamics. Strains showing changes in growth were further investigated to identify potential mechanisms behind any observed adverse growth impacts. This approach enhanced knowledge of toxicity impacts, potential for microbiome imbalance (dysbiosis) and associated consequences for host health arising from exposure to a group of emerging pollutants of recent environmental interest.

Material and Methods

Selected Tire Derived Compounds

Pure compounds of selected tire wear derived chemicals (Table 1) were used for high-throughput growth inhibition assay. Screened concentrations for benzothiazoles ranged from 1 ng/L to 10 mg/L in 10-fold serial dilutions (1 ng/L, 10 ng/L, 100 ng/L, 1 µg/L, 10 µg/L, 100 µg/L, 1 mg/L, and 10 mg/L), while for DPG, concentrations ranged from 10 ng/L to 100 mg/L (10 ng/L, 100 ng/L, 1 µg/L, 10 µg/L, 100 µg/L, 1 mg/L, 10 mg/L, 50 mg/L and 100mg/L).

Table 1: Selected tire wear derived organic compounds tested for growth impact on representative bacterial gut strains

Group	Full Name	Abbreviation	Supplier	Structure (https://www.sigmaaldrich.com)
Benzothiazoles	2-mercaptobenzothiazole	MBT	Sigma-Aldrich	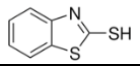
	5-methyl-1H-benzotriazole	MHBT	Sigma-Aldrich	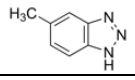
Others	1,3-diphenylguanidine	DPG	Sigma-Aldrich	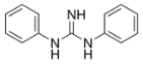

Preparation of Medium

To cultivate the bacteria used for screening, Brain Heart Infusion (BHI) broth was prepared according to manufacturer's instructions and sterilised by autoclaving. Briefly, 18.5 g of BHI powder was weighed and added to 500 mL of Millipore Q water to prepare 500 mL of broth (pH 7.5, ±0.2).

Inoculation and Incubation of Pure Cultures

Bacterial strains used in this study (Table 2) were obtained from the DSMZ (German Collection of Microorganisms and Cell Cultures GmbH) or an in-house collection at the Division of Microbial Ecology, Centre for Microbiology and Environmental Systems Science, University of Vienna.

These strains were selected based upon both prevalence and abundance in the healthy gut of humans to represent the core microbiome as well as capture some key microbial metabolic processes (e.g. fermentation, sulfidogenesis).

Table 2: Bacterial strains from the human gut used in this study. (T), indicates type strain.

Name	Strain	NCBI Sequence
Alistipes putredinis	DSM 17216 (T)	ABFK00000000.2

Akkermansia muciniphila	DSM 22959 (T)	NC_010655.1
Bacteroides caccae	DSM 19024 (T)	GCA_028539535.1
Bacteroides fragilis	DSM 2151 (T)	NC_003228.3/CR626927.1
Bacteroides xylanisolvens	DSM 18836 (T)	FP929033.1
Collinsella aerofaciens	Fecal isolate	Not available
Escherichia coli	Fecal isolate	Not available
Enterocloster bolteae	DSM 15670 (T)	ABCC00000000.2
Enterococcus faecium	Brno hospital isolate	Not available
Lactobacillus hominis	DSM 23910 (T)	CAKE01000000

Inoculations and incubations of all bacterial cultures were performed under anaerobic conditions (85% N_2, 10% CO_2, 5% H_2) in an anaerobic chamber (Coy Laboratory Products, USA). Liquid cultures were inoculated into pre-reduced (24H) 10 mL of Brain Heart Infusion (BHI) medium (Table 3), incubated for 20-24 hours, at 37 ºC overnight (ON), and the optical density (OD) at 600 nm was measured prior to dilution. To ensure consistency across species, the OD_{600} of all overnight cultures was adjusted to 0.01 prior to the beginning of the experiments.

Table 3: Brain Heart Infusion media composition, given in grams per liter of medium

Brain Heart Infusion (BHI) broth composition	g/L
Beef heart	5
Calf brains	12.5
Disodium hydrogen phosphate	2.5
D(+)-glucose	2
Peptone	10
Sodium chloride	5
Final pH (at 25°C)	7.4

Sequencing of pure strains

To confirm the identity of the pure cultures used in the analyses, 500–1,000 µL of overnight cultures were harvested under atmosphere-controlled conditions and centrifuged at 13,000 × g for 5 min. The supernatant was discarded, and the pellet was resuspended in 50 µL of Nuclease Free water. Subsequently, DNA was extracted using FASTDNA Spin Kit for Soil (MP Biomedical) according to maufacturers instructions. The purified DNA was transferred to sterile microcentrifuge tubes and stored at -20°C until further analysis.

To amplify the 16S rRNA gene from the extracted DNA samples, PCR was performed. Each reaction contained 22 µL of nuclease-free water, 1 µL of forward primer (27F), 1 µL of reverse primer (1492R), 1 µL of DNA template, and 25 µL of DreamTaq Master Mix (Thermo Fisher Scientific), for a total reaction volume of 50 µL. The PCR thermal cycling conditions used for amplification of the 16S rRNA gene are summarized in Table 4.

Table 4: PCR cycling conditions used for amplification of the bacterial 16S rRNA gene

Temerature (C°)	Time	Phase
95	3 min	Initial denaturation
95	30 s	30 cycles
52	30 s	
72	90 s	
72	10 min	Final elongation
12	∞	Cooling

In order to check DNA quality a 1% agarose gel was prepared. In 1× TAE running buffer samples were loaded along with 1 kb DNA ladder (GeneRuler, Thermo Fisher Scientific). Electrophoresis was performed at 100 V for 45 minutes. The gel was then visualized using a Bio-Rad (Bio-Rad Laboratories GesmbH, Austria) gel documentation system. PCR products were further purified using the InnuPREP PCRpure Purification Kit (Innuscreen GmbH) according to the manufacturer's instructions. Following the final centrifugation step, 15 µL of elution buffer was added, incubated at room temperature and centrifuged to obtain the purified product. DNA concentration was measured using a NanoDrop spectrophotometer (Thermo Fisher Scientific). Samples were diluted for sequencing to a final DNA concentration of ~50 ng/µL in a total volume of 15 µL. Sanger sequencing was performed by Microsynth Austria GmbH (Vienna, Austria). The resulting sequences were visualized and manually trimmed to remove low-quality regions using A plasmid Editor (ApE) tool (Davis, 2022). Strain identity was confirmed using the NCBI BLAST tool with a similarity cutoff >97% (Boratyn, 2013).

High-Throughput Growth Inhibition assay of Benzothiazoles and 1,3-diphenylguanidine (DPG) on Gut Microbiota Growth

For the preparation of the master plate, compounds were dissolved in DMSO at 100x the screening concentration. To automate the process and test multiple concentrations and pollutants per plate, a master plate was prepared according to a predetermined layout before preparing the medium plates. The experimental flow is depicted in the Figure 7.

To prepare medium plates 98 µl of BHI medium was added to each well of a 96 well plate (Greiner, Sigma-Aldrich). Following this, pollutants were transferred from the master plate to the medium, with 2 µl added per well (representing a 100-fold dilution). Plates were introduced to anaerobic chamber where 100 µl of bacteria from overnight cultures diluted to OD_{600}=0.01, or medium (for blank controls), were added to each well for a final compound concentration ranging from 1 ng/L to 10 mg/L and 10 ng/L to 100 mg/L for benzothiazoles and DPG, respectively, and a final DMSO concentration of 1% in all wells. Additionally, a solvent control (1% DMSO) and an antibiotic control (Clindamycin, 0.1 µg/mL; Alfa Aesar) were included to to ensure that any changes in bacterial growth were not associated with the vehicle (solvent, DMSO) and could be linked to the compound itself and the antibiotic serving to confirm the functionality and sensitivity of the assay through a known growth-inhibitory compound. A layout example for benzothiazoles is depicted in Table 5.

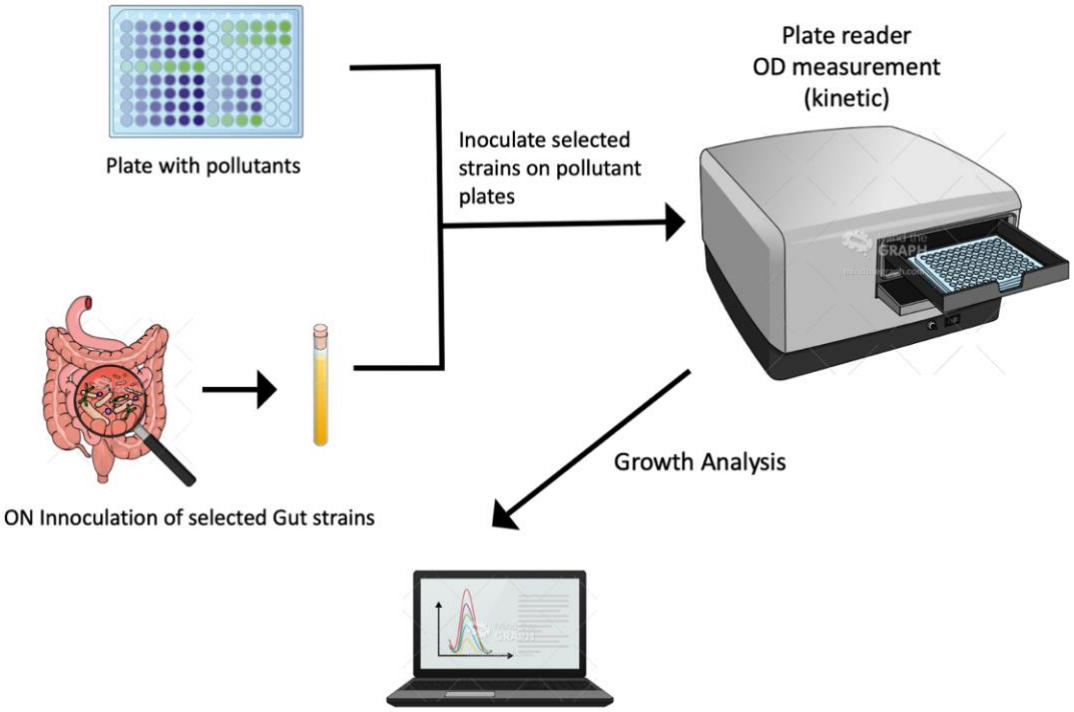

Figure 7: Experimental workflow of the high-throughput growth inhibition assay used to assess the effects of TWPs-derived compounds on representative human gut bacterial strains.
Selected gut bacterial strains were cultured over night (ON) and after dilution inoculated into microplates containing test compounds, including 2-mercaptobenzothiazole (MBT), 5-methyl-1H-benzotriazole (MHBT), and 1,3-diphenylguanidine (DPG), across a wide concentration range. Following inoculation, bacterial growth was monitored kinetically using a microplate reader through optical density (OD_{600}) measurements. Growth data were subsequently analyzed to evaluate changes in growth dynamics, including lag phase duration, growth rate, area unter the curve (AUC) etc., enabling the assessment of concentration-dependent and strain-specific responses to TWPs-derived compounds. Figure created in Mind the Graph (mindthegraph.com).

Following bacterial addition, plates were sealed with a gas permeable membrane (Breathe-Easy, Merck) and stacked using a stacker (Biostack4, Agilent BioTek) and the OD_{600} measured every 20 minutes for a total of 24 hours using a plate reader (Epoch2, Agilent BioTek). Full plate reader settings are detailed in Table 6. Each experiment includes three independent biological replicates, with each having at least 4 technical replicates per condition to ensure data reliability and reproducibility.

Due to the inclusion of multiple gut strains within the same experimental setup, a standardized 24 h kinetic measurement was applied, as the majority of strains exhibited all phases of growth within this timeframe. Consequently, for some slower-growing strains, only the lag and exponential phases were captured during the initial run. For strains in which growth inhibition was observed, the assay duration was extended until the stationary phase was reached to ensure comprehensive evaluation of treatment effects.

Table 5: An example of the layout for growth inhibitory concentration experiments, where strain 1 refers to one of the selected gut strains eg. *A. rectalis* and strain 2 to another eg. *B. xylanisolvens,*
SOL= solvent DMSO control, AB ctrl=antibiotic control (Clindamycin,0.01 µg */mL), Blank= media/blank control*

	Strain 1						Strain 2					
	1	2	3	4	5	6	7	8	9	10	11	12
A	10 mg/L	10 mg/L	10 mg/L	10 mg/L	SOL	SOL	10 mg/L	10 mg/L	10 mg/L	10 mg/L	SOL	SOL
B	1 mg/L	1 mg/L	1 mg/L	1 mg/L	SOL	SOL	1 mg/L	1 mg/L	1 mg/L	1 mg/L	SOL	SOL
C	100 µg/L	100 µg/L	100 µg/L	100 µg/L	AB ctrl	AB ctrl	100 µg/L	100 µg/L	100 µg/L	100 µg/L	AB ctrl	AB ctrl
D	10 µg/L	10 µg/L	10 µg/L	10 µg/L	AB ctrl	AB ctrl	10 µg/L	10 µg/L	10 µg/L	10 µg/L	AB ctrl	AB ctrl
E	1 µg/L	1 µg/L	1 µg/L	1 µg/L	Blank	Blank	1 µg/L	1 µg/L	1 µg/L	1 µg/L	Blank	Blank
F	100 ng/L	100 ng/L	100 ng/L	100 ng/L	Blank	Blank	100 ng/L	100 ng/L	100 ng/L	100 ng/L	Blank	Blank
G	10 ng/L	10 ng/L	10 ng/L	10 ng/L	Blank	Blank	10 ng/L	10 ng/L	10 ng/L	10 ng/L	Blank	Blank
H	1 ng/L	1 ng/L	1 ng/L	1 ng/L	Blank	Blank	1 ng/L	1 ng/L	1 ng/L	1 ng/L	Blank	Blank

Table 6: Experimental settings for plate reader measurements

Parameter	**Setting/Value**
Temperature	37 °C with a 1 °C gradient
Number of Cycles	73 cycles
Cycle Duration	~20 minutes per cycle
Total Duration	24 hours
Shaking Type	Orbital motion
Shaking Duration	10 seconds (0:00:10) before each measurement
Shaking Frequency	425 cycles per minute (cpm)
Shaking Radius	3 mm
Measurement Wavelength	600 nm (Absorbance)
Read Speed	Normal
Delay Between Data Points	100 milliseconds
Measurement Type	Full plate, endpoint absorbance at each cycle

Trace Metal Supplementation Assay

To address the metal chelation hypothesis, whereby benzothiazoles may induce growth delay or inhibition through sequestration of essential trace metals, supplementation with the trace mineral solution MD-TMS (ATCC) (Table 7) was performed in wells containing a concentration range of MBT/MHBT (1 ng/L–10 mg/L). As this supplement is commonly used to support bacterial growth, including numerous gut strains, at a concentration of 10 mL/L (Korth, 2024; Kijner, 2024; Zhou, 2024), higher concentrations were tested to evaluate a potential rescue effect through increased metal availability. The same controls were applied as previously described, including a solvent control (1% DMSO) to verify that the solvent did not affect bacterial growth, Blank/only medium control and an antibiotic control (Clindamycin, 0.1 µg/mL; Alfa Aesar) to confirm assay performance through a reproducible inhibitory response.

MD-TMS was added to BHI at final concentrations of 20 and 30 mL/L. As previously described, 98 µL of BHI supplemented with MD-TMS and 2 µL of the respective pollutant concentration, DMSO, or antibiotic (Clindamycin) control and Blank controls were added to the designated wells according to the predetermined layout. Subsequently, 100 µL of *C. aerofaciens* inoculum (OD_{600} = 0.01) was added to each well, and the experiment was conducted as previously described). Bacterial growth was compared with the solvent control, which was set as the maximum growth (100%); however, growth values were not cut off at this level, which allowed for the detection of growth exceeding the control. The assay included three biological replicates, each containing four technical replicates per treatment condition.

Table 7: Composition of the trace mineral solution used for supplementation assays, based on Wolfe's formulation (https://www.atcc.org/products/md-tms). Concentrations are given in g/L.

Component	**Concentration (g/L)**
EDTA	0.5
$MgSO_4 \cdot 7H_2O$	3
$MnSO_4 \cdot H_2O$	0.5
NaCl	1
$FeSO_4 \cdot 7H_2O$	0.1
$Co(NO_3)_2 \cdot 6H_2O$	0.1
$CaCl_2$ (anhydrous)	0.1
$ZnSO_4 \cdot 7H_2O$	0.1
$CuSO_4 \cdot 5H_2O$	0.01
$AlK(SO_4)_2$ (anhydrous)	0.01
H_3BO_3	0.01
$Na_2MoO_4 \cdot 2H_2O$	0.01
Na_2SeO_3 (anhydrous)	0.001
$Na_2WO_4 \cdot 2H_2O$	0.01
$NiCl_2 \cdot 6H_2O$	0.02

Automated Microbial Growth Analysis, Statistics, and Visualization

Raw data from the plate reader (Epoch2, Agilent BioTek) were initially processed using Software for Automated Analysis of Microbial Growth Assays (AMiGA s)oftware (Midani, 2021), which performed curve fitting and generated summary files. For further analysis, only the Area Under the Curve (AUC), including empirical, logarithmic, and linear values, and LagP and LagC (the time delay required to enter exponential growth and initiate positive growth, respectively) were extracted from the summary files. Technical replicates (at least four per plate) were pooled and mean values for each pollutant concentration were calculated for each biological replicate. Outliers among technical replicates within each biological replicate were excluded when coefficient of variation (CV) calculated exceeds the threshold of 0.2 (20% variation) ensuring the reliability of the final dataset. The final plotted values were calculated as the mean of independent biological replicates, providing that at least two out of the three produced comparable data, using the linear Area Under the Curve (AUC_{lin}) as the evaluated growth parameter. An antibiotic control (Clindamycin, 0.1 µg/mL; Alfa Aesar) was included to evaluate potential growth inhibition. In the growth inhibition assay, a 20% reduction in growth relative to the solvent control was used as the threshold to define inhibitory effects (Lindell A. E.-K., 2022). A Blank control (medium only) was also included to assess contamination and enable data normalization; absorbance values from blank wells were subtracted from those of treatment wells to determine growth inhibition accurately. Heatmaps were generated in R using the ggplot2 package (Wickham H. , 2011) to display AUC_{lin} values across isolates and concentrations as percentages. AUC_{lin} was selected over logarithmic values, as it better represents biomass without obscuring extreme values. For each strain, the inhibition percentage was calculated relative to the relevant solvent control (DMSO), which was assigned a value of 100%, ensuring comparability between strains. Heatmaps for the 24 h MD-TMS supplementation assay and the 72 h benzothiazole exposure assay with *C. aerofaciens* were generated similarly using ggplot2 (Wickham H. , 2011), based on AMiGA-processed growth data and subjected to the same downstream processing criteria described above (filtering, averaging, replicate selection). Statistical comparisons of each concentration versus the solvent control were performed using Welch's two-sample t-test based on independent biological replicates, followed by Benjamini–Hochberg correction for multiple comparisons (Welch, 1947; Benjamini, 1995).

Additionally, growth curve data from benzothiazole treatments and benzothiazole treatments supplemented with trace minerals (MD-TMS) were processed and visualized in R using the tidyverse package (Wickham H. M., 2019). For comparative visualization, data from the 72 h benzothiazole exposure assay were truncated to the first 24 h to enable direct comparison with the 24 h MD-TMS supplementation assay and observation of early growth dynamics. Raw OD_{600} values were normalized by subtracting the corresponding blank control value at each time point from all treatment conditions. Because recorded time values varied slightly between replicates, the mean time across replicates was used for each measurement point. For each treatment, mean normalized OD_{600} and standard deviation (SD) across biological replicates were calculated at aligned time point (using the same criteria: at least two of three biological replicates produced comparable results). Growth curves were generated using ggplot2 (Wickham H. , 2011) as line plots with overlaid data points and shaded ribbons representing mean ± SD.

Results

16S rRNA Sequencing Confirmed the Identity of All Pure Gut Bacterial Strains

Table 8: Sequenced strains and percentage identity and Accessionnumber based on NBCI BLAST analysis

Name	% identity	Accession
Akkermansia muciniphila	98.87	CP029700.1
Alistipes putredinis	100.00	NR_025909.1
Bacteroides caccae	99.83	NR_112932.1
Bacteroides fragilis	99.80	CR626927.1
Bacteroides xylanisolvens	99.91	NR_112947.1
Collinsella aerofaciens	99.46	PQ236811.1
Escherichia coli	99.31	MZ964587.1
Enterocloster bolteae	100.00	CP094684.1
Enterococcus faecium	99.91	MW135213.1
Lactobacillus hominis	99.66	LC589211.1

Sanger sequencing of the 16S rRNA gene amplicons was utilized to confirm the taxonomic identity of all analyzed strains (Table 8). Sequence comparison using NCBI BLAST revealed high identity values ranging from 98.87% to 100% relative to reference sequences in the database (Boratyn, 2013). *Enterocloster bolteae* and *Alistipes putredinis* showed 100% identity, while the remaining strains, exhibited ≥98.8% sequence similarity to their respective reference strains. These results confirm the correct species and strain-level identification of the bacterial isolates used in subsequent experiments.

High-Throughput Growth Inhibition assay of Reveales Strain-Specific Responses of Gut Microbiota to Benzothiazoles and 1,3-diphenylguanidine (DPG)

A high-throughput anaerobic growth inhibition assay was conducted to assess the effects of tire wear particles (TWPs)-derived compounds on representative human gut bacterial strains. Pollutants dissolved in DMSO were added into brain-heart infusion medium in 96-well plates, which were inoculated with diluted overnight cultures (OD_{600} = 0.01), and incubated anaerobically with appropriate controls. Bacterial growth was monitored kinetically by measuring OD_{600} every 20 min for 24 h using a plate reader. The Area Under the Curve (AUC) growth parameter used to determine strain-specific responses to selected TWPs-related compounds.

Among the tested isolates, only *Collinsella aerofaciens* exhibited consistent inhibition in response to both MBT and MHBT. For MBT (Figure 8), inhibition was first observed at 100 ng/L and remained consistent up to 10 mg/L, with values ranging between 20–30%, indicating a non-concentration-dependent effect. Statistical comparisons versus solvent control showed that no MBT treatment concentration remained significant after Benjamini–Hochberg correction across the tested strains (adjusted $p > 0.05$), although *C. aerofaciens* displayed the

strongest inhibitory trend based on mean growth reduction, with consistent inhibition observed across all biological replicates.

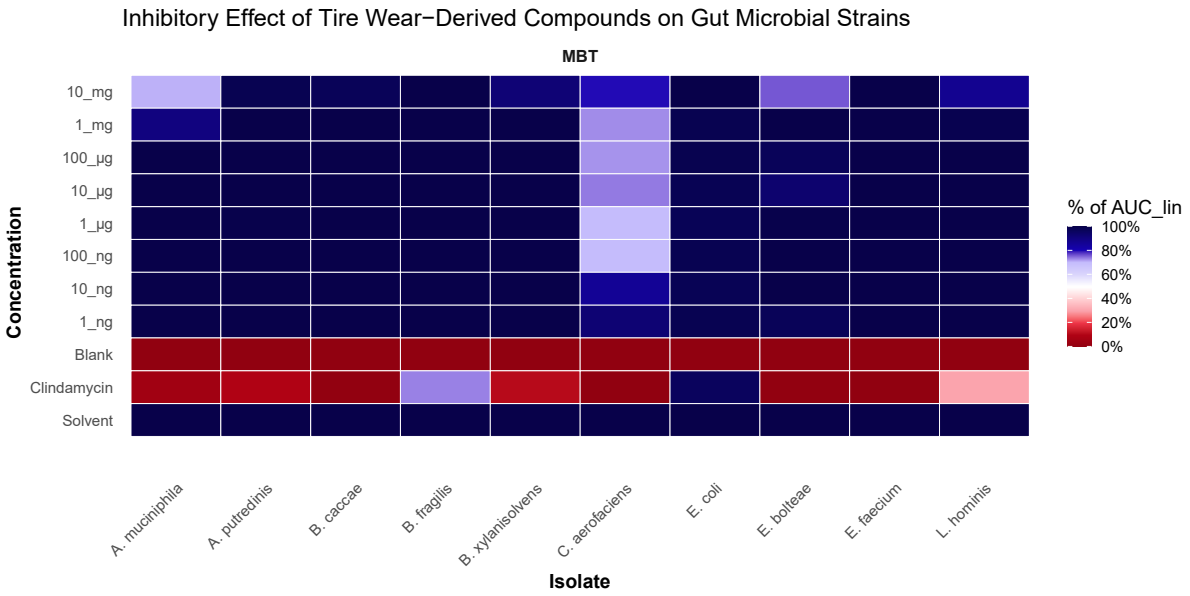

Figure 8: Heatmap of complete growth inhibition assay results for MBT across 10 representative gut bacterial strains.
To assess the effects of representative TWPs-derived compounds, namely MBT a high-throughput growth inhibition assay was conducted. Growth kinetics were monitored over 24 hours, with OD_{600} measured every 20 minutes using a plate reader (Epoch2, Agilent BioTek) under anaerobic conditions. Relative growth of three independent biological replicates (each including 4 technical replicates) (%AUC_lin) was averaged and normalized to the solvent control (DMSO = 100%). Rows represent MBT concentrations (1 ng/L–10 mg/L) and columns represent individual isolates. The Blank (medium only) control confirmed the absence of contamination, while antibiotic (Clindamycin) and Solvent controls were included for comparison and validation of assay performance. Color intensity indicates inhibition, where dark blue indicates high growth (80% or greater), corresponding to no relevant inhibition (less than 20% of inhibition), whereas values below 80% growth (purple to red) indicate increasing levels of growth inhibition. While *C. aerofaciens* and to a lesser extant *A . muciniphila* and *E. bolteae* showed reduced mean growth at several concentrations, within each biological replicate, no statistically significant differences were detected after correction ($p > 0.05$).

MHBT demonstrated effects against *C. aerofaciens* at an even lower concentration of 10 ng/L (Figure 9), with consistent inhibition maintained up to 1 mg/L. However, at the highest tested concentration (10 mg/L), inhibition dropped slightly below the threshold of biological relevance, nearing 20%. Here, as with MBT, inhibition was not concentration dependent but remained consistent, ranging between 20–26% across effective concentrations.

Similarly, *Akkermansia muciniphila* exhibited approximately 30% and slightly over 32% growth inhibition, following exposure to both MBT and MHBT, respectively, at the highest tested concentration (10 mg/L). Regarding *Enterocloster bolteae*, MHBT treatment resulted in a consistent growth reduction of approximately 15–19% across nearly all tested concentrations; however, this did not exceed the predefined biologically relevant threshold, while MBT treatment inhibited growth solely at 10 mg/L, with inhibition nearing 25%. Further, *Lactobacillus hominis* exhibited slight growth reduction at 10 mg/L, with MBT and MHBT

causing approximately 14% and 18% inhibition, respectively, both below the defined biological significance threshold. All other strains, including *A. putredinis*, *B. caccae*, *B. fragilis*, *B. xylanisolvens*, *E. coli*, and *E. faecium*, were not affected by MBT and MHBT across the full concentration range. Statistical comparisons versus solvent control showed that no MHBT treatment concentration remained significant after Benjamini–Hochberg correction across the tested strains ($p > 0.05$), althoug growth reduction trends were observed in selected taxa (within each biological replicate), particularly *C. aerofaciens* and *A. muciniphila*.

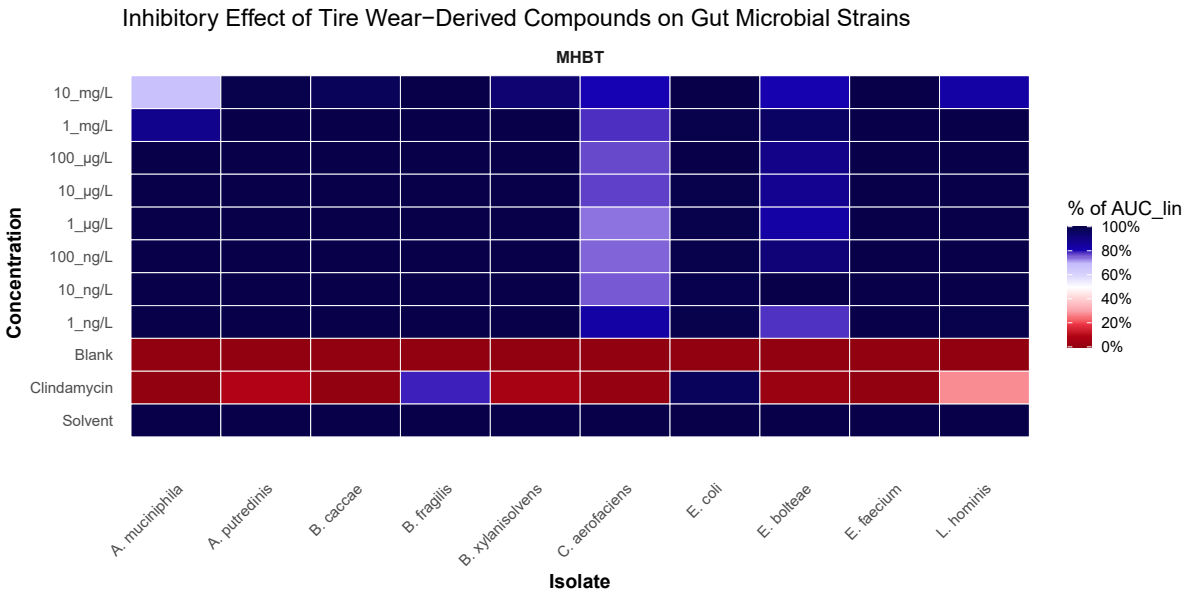

Figure 9: Heatmap of complete growth inhibition assay results for MHBT across 10 representative gut bacterial strains.
To assess the effects of representative TWPs-derived compounds, namely **MHBT** a high-throughput growth inhibition assay was conducted. Growth kinetics were monitored over 24 hours, with OD_{600} measured every 20 minutes using a plate reader (Epoch2, Agilent BioTek) under anaerobic conditions. Relative growth of 3 independent biological replicates replicates (each including 4 technical replicates) (% AUC_lin) was averaged and normalized to the solvent control (DMSO = 100%). Concentrations range is from 1 ng/L to 10 mg/L. The Blank (medium only) control confirmed the absence of contamination, while antibiotic (Clindamycin) and Solvent controls were included for comparison and validation of assay performance. Color intensity reflects the degree of growth inhibition, where dark blue indicates high growth (80% or greater), corresponding to no relevant inhibition (less than 20% of inhibition), whereas values below 80% growth (purple to red) indicate increasing levels of growth inhibition. While *C. aerofaciens* and to a lesser extent *A. muciniphila* showed reduced mean growth at several concentrations, no statistically significant differences were detected after correction. ($p > 0.05$).

Additionally, blank (medium only) controls (Blank) were representative, with no contamination, while solvent (DMSO) controls (Solvent) showed no inhibitory effects, confirming the neutrality of the solvent. The antibiotic control (Clindamycin) functioned as expected for most strains, except *E. coli* and to a lesser extent *B. caccae*, which demonstrated some resistance, in line with previous observations (Nyberg, 2007). Importantly, the initial OD for all strains was standardized to 0.01, allowing clear visualization of lag phases and early

growth dynamics of majority of tested strains. These results show that *C. aerofaciens* is selectively susceptible to MBT and, to a higher extent, MHBT, while the growth of remaining strains appeared mostly unaffected by either compound under the tested conditions.

The effects of DPG on bacterial growth were also assessed using the same ten strains (Figure 10) over a concentration range from 10 ng/L to 100 mg/L. Growth inhibition was observed only in two strains, *A. muciniphila* and *C. aerofaciens*, and only at the highest concentrations tested (100 and 50 mg/L). For *A. muciniphila*, growth inhibition was approximately 53% at 100 mg/L and around 27% at 50 mg/L, while *C. aerofaciens* showed growth inhibition only at 100 mg/L, with a reduction of just over 20%. However, no statistically significant differences were detected after correction ($p > 0.05$).

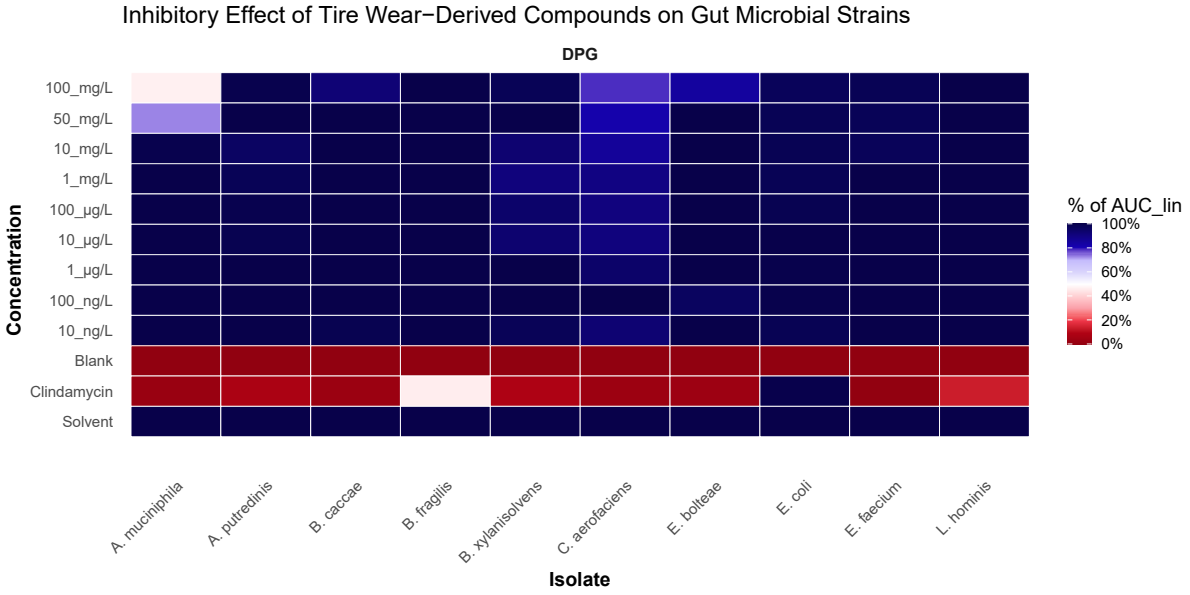

Figure 10: Heatmap of complete growth inhibition assay results for DPG across 10 representative gut bacterial strains.
To assess the effects of representative TWPs-derived compounds, namely **DPG** a high-throughput growth inhibition assay was conducted. Growth kinetics were monitored over 24 hours, with OD_{600} measured every 20 minutes using a plate reader (Epoch2, Agilent BioTek) under anaerobic conditions. Relative growth of three independent biological replicates (each including 4 technical replicates) (% AUC_lin) was averaged and normalized to the solvent control (DMSO = 100%). Concentrations range is from 1 ng/L to 100 mg/L, while the Blank (medium only) control confirmed the absence of contamination, and antibiotic (Clindamycin) and Solvent controls were included for comparison and validation of assay performance. Color intensity reflects the degree of growth inhibition, where dark blue indicates high growth (80% or greater), corresponding to no relevant inhibition (less than 20% of inhibition), whereas values below 80% growth (purple to red) indicate increasing levels of growth inhibition. While *A . muciniphila* showed reduced mean growth at several concentrations, no statistically significant differences were detected after correction. (adjusted $p > 0.05$).

Trace Mineral Supplementation Mitigates the Growth-Inhibitory Effects of Benzothiazoles in *C. aerofaciens*

To further investigate the consistent inhibitory effects of MBT and MHBT on *C. aerofaciens*, a trace mineral supplementation assay was performed by adding MD-TMS to the benzothiazole growth inhibition assay. One proposed mechanism was that benzothiazoles may chelate essential trace metals, thereby limiting metal availability required for enzymatic activity and cellular metabolism. As *C. aerofaciens* was the only strain exhibiting significant consistent growth inhibition following benzothiazole treatment growth dynamics were examined in more detail (Figure 11A; Figure12A). Analysis focused on the first 24 h of growth (lag and partial exponential phase) extracted from a prolonged ~72 h run, while a separate 24 h assay supplemented with additional trace minerals was performed to assess whether the observed growth delay and inhibition were mitigated.

Treatment with MBT resulted in a slight variation in lag-phase compared to the solvent control, resulting in a reduced slightly overall yield (Figure 11A). Following supplementation with 20 and 30 mL/L of trace mineral supplement (standard use to support microbial growth is 10 mL/L), this slight inhibition was no longer observed (Figure 11B). Because MD-TMS supplement contains several metal ions that may be complexed by benzothiazoles, including Co^{2+} (0.1 g/L as $Co(NO_3)_2 \cdot 6H_2O$), Ca^{2+} (0.1 g/L as $CaCl_2$), Zn^{2+} (0.1 g/L as $ZnSO_4 \cdot 7H_2O$), Cu^{2+} (0.01 g/L as $CuSO_4 \cdot 5H_2O$), Ni^{2+} (0.02 g/L as $NiCl_2 \cdot 6H_2O$), molybdate (0.01 g/L as $Na_2MoO_4 \cdot 2H_2O$),and selenite (0.001 g/L as Na_2SeO_3), the restored growth suggests that increased mineral availability compensated for reduced metal bioavailability. A similar rescue pattern was observed for MHBT (Figure 12A;B). Consistent with these observations, no growth inhibition was detected in AUC linear values after 24 h in the presence of trace minerals in any of the three independent biological replicates (Figure 13). At the maximum tested dose (10 mg/L), MBT and MHBT corresponed to approximately 59.8 µM and 75.1 µM, respectively, whereas MD-TMS supplementation yielded a total nominal trace metal concentration of approximately 346 µM at 20 mL/L and 520 µM at 30 mL/L, indicating that trace metals were supplied in substantial molar excess over both compounds.

Final mean AUC_{lin} values were calculated using biological replicates that showed comparable growth behavior, with at least two of three independent biological replicates (each comprising four technical replicates) required for inclusion in the final analysis. Statistical analysis of *C. aerofaciens* growth curves confirmed significant MBT-associated growth inhibition at 10 mg/L and 1 mg/L following Benjamini–Hochberg correction ($p = 0.0037$ and $p = 0.041$, respectively), while 100 µg/L narrowly missed the significance threshold ($p = 0.0505$). In contrast, no MHBT concentration reached statistically significant inhibition after correction, although 1 mg/L showed the strongest inhibitory trend ($p= 0.079$). Following trace mineral supplementation, no treatment condition showed formal significant growth differences comparing to solvent; however, near-significant increases in growth were observed for MBT at 10 ng/L ($p = 0.053$) and for MHBT at 1 µg/L ($p= 0.089$), indicating partial rescue of compound-associated growth inhibition. This supports the hypothesis that the observed effects are potentially linked to metal chelation by benzothiazoles as opposed to toxic mechanisms of the compound itself.

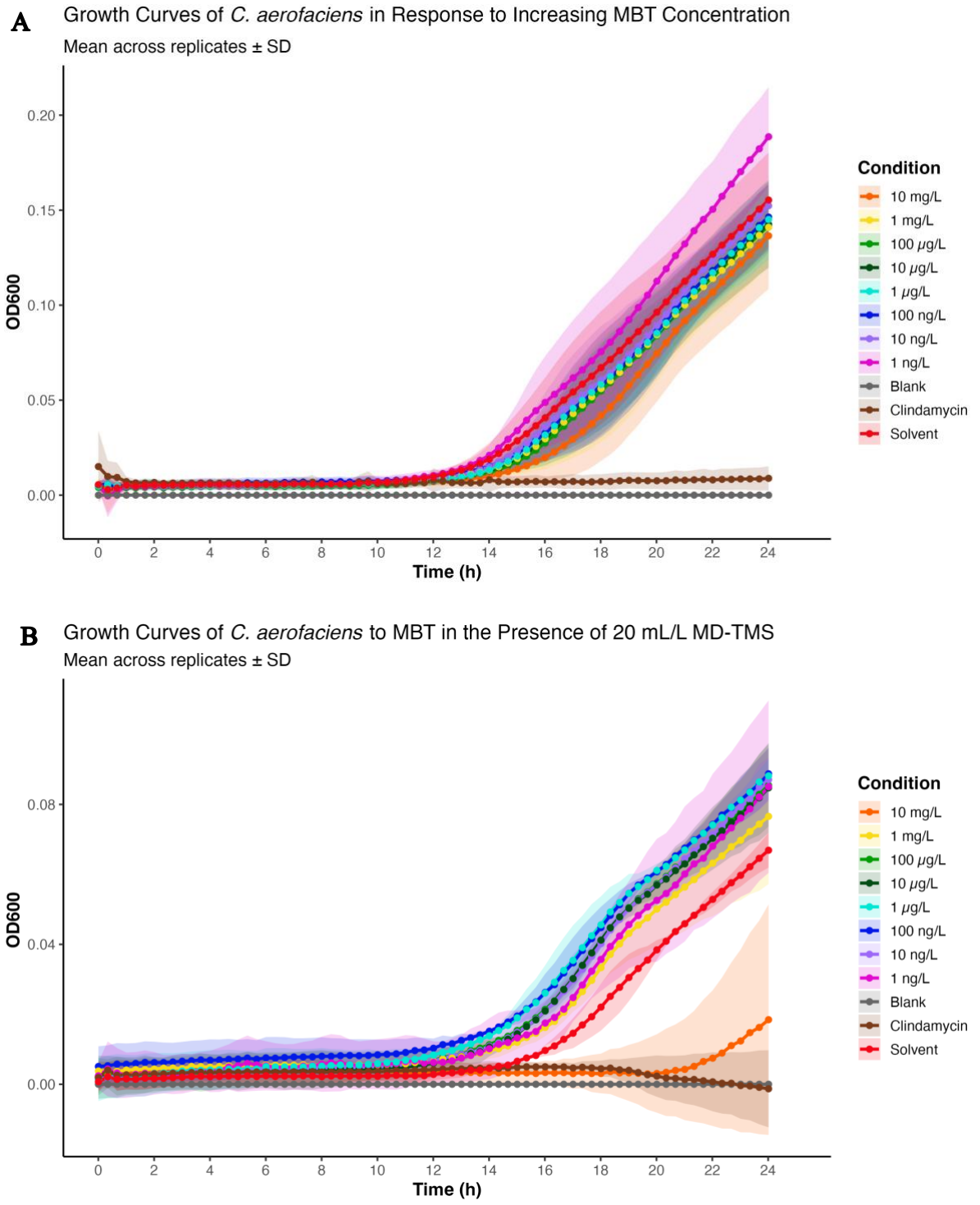

Figure 11 (A): Growth curves of *C. aerofaciens* under 2-mercaptobenzothiazole (MBT) treatment. Growth of *C. aerofaciens* (OD_{600}) over time across a range of MBT concentrations (1 ng/L–10 mg/L). Across all tested concentrations with exception of 1 ng/L, growth curves for most concentrations show slight delay in growth, following closely the solvent control, with minor variations in lag phase, without a clear concentration-dependent trend. Following this delay, treated cultures reach slightly reduced growth levels, and overall AUC, comparing to the control. However, significant growth inhibition was observed at 10 mg/L and 1 mg/L ($p < 0.05$), while 100 µg/L showed borderline significance following correction ($p = 0.0505$). All

remaining concentrations were not statistically significant ($p \geq 0.05$). The antibiotic (Clindamycin) control shows complete growth inhibition, while blank control shows no growth ensuring no detectable contamination. These results indicate that MBT primarily affects early growth kinetics rather than overall growth capacity. **(B): Growth curves of *C. aerofaciens* under 2-mercaptobenzothiazole (MBT) treatment and trace mineral supplementation (20mL/L).** Growth of *C. aerofaciens* (OD_{600}) over time across a range of MBT concentrations (1 ng/L–10 mg/L) in the presence of trace minerals (TMS-MD). Compared to untreated conditions, the previously observed slight lag-phase delay and inhibition are no longer apparent. Most treatments resulted in a comparable biomass to the solvent, indicating that trace mineral supplementation alleviates the inhibitory effect of MBT. Only the highest concentration shows reduction in growth, with no statistically significant dicrease in growth after correction. Further, 10 ng/L narrowly missed the threshold ($p = 0.053$), while 1 µg/L showed a trend toward increased growth ($p = 0.078$). The antibiotic (Clindamycin) control remains inhibited, while the blank control shows no growth.

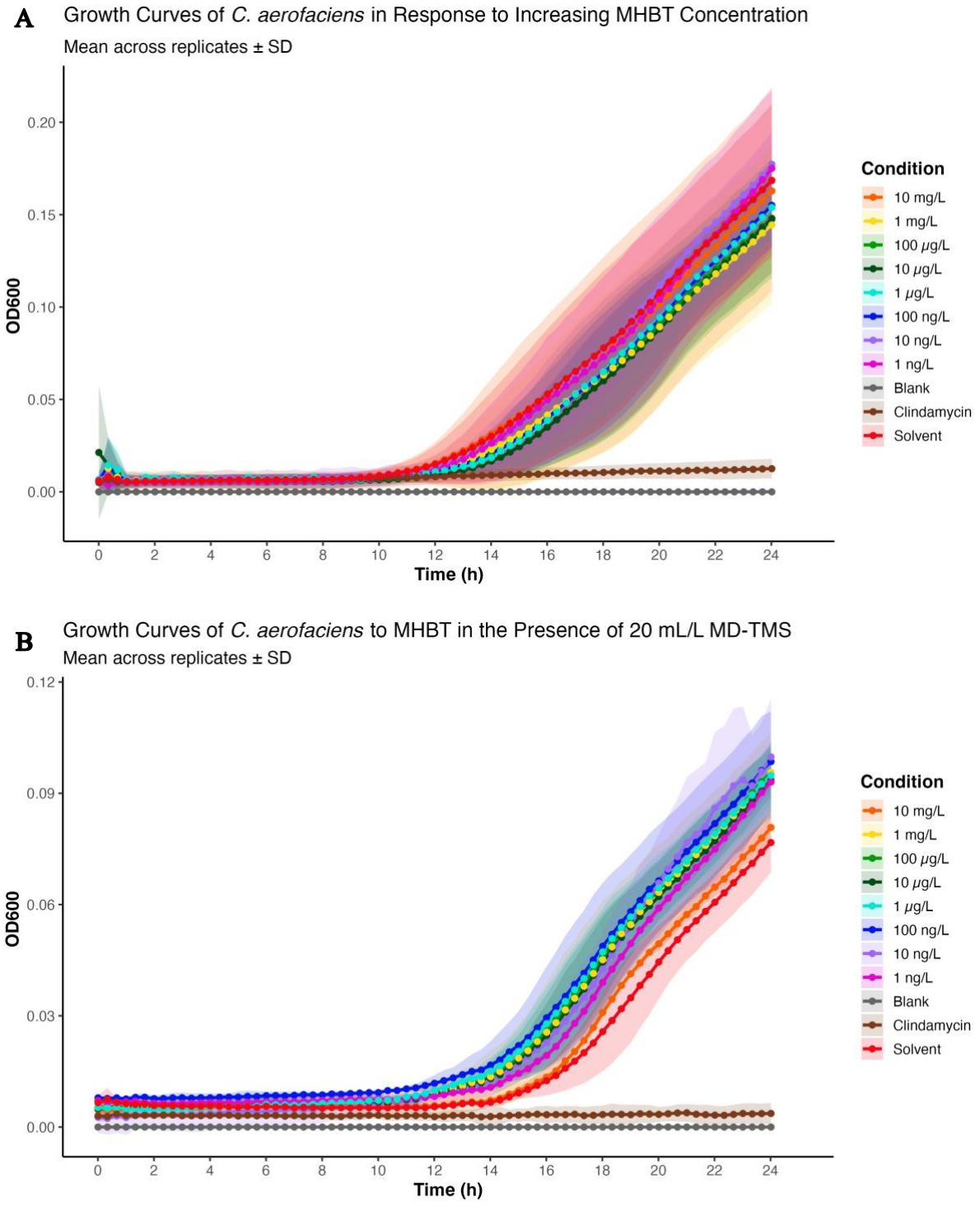

Figure 12 (A): Growth curves of *C. aerofaciens* under 5-methyl-1H-benzotriazole (MHBT) treatment. Growth of *C. aerofaciens* (OD_{600}) over time across a range of MHBT concentrations (1 ng/L–10 mg/L). A slight delay in the onset of exponential growth is observed across treatments compared, with exception of 1 ng/L, 10 ng/L and 10 mg/L whose grwth curve overlap with the solvent control, with no MHBT treatment concentration reaching statistical significance after correction. However, 1 mg/L ($p = 0.079$), 100 µg/L ($p = 0.120$), and 10 µg/L ($p = 0.134$) showed trends toward reduced growth. The antibiotic control (Clindamycin) shows inhibited growth, while the blank control shows no growth, indicating that MHBT primarily affects early growth dynamics without causing sustained inhibition. **(B): Growth curves of *C.***

***aerofaciens* under 5-methyl-1H-benzotriazole (MHBT) treatment with trace mineral supplementation (20 mL/L).** Growth of *C. aerofaciens* (OD_{600}) over time across a range of MHBT concentrations (1 ng/L–10 mg/L) in the presence of trace minerals (TMS-MD). Compared to untreated conditions, no trend towards delay in the onset of exponential growth is observed, and growth is slightly higher relative to the solvent control with no statistically significant growth differences after correction. However, 1 µg/L showed the strongest trend toward increased growth ($p = 0.089$), with similar near-significant effects at 100 µg/L, 10 µg/L, and 10 ng/L ($p = 0.090$), suggesting partial rescue under MHBT exposure. The antibiotic control (Clindamycin) remains inhibited, while the blank control shows no growth, indicating that trace mineral supplementation mitigates the previously observed effects of MHBT.

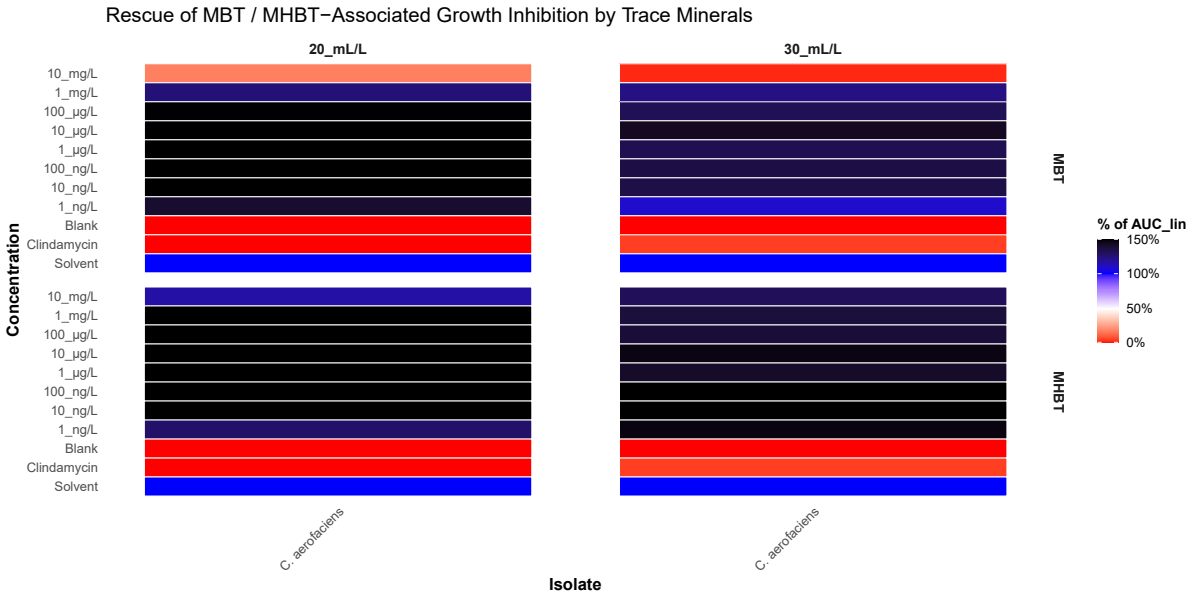

Figure 13: Rescue of benzotiazole-associated growth inhibition of *C. aerofaciens* with trace minerals supplementation. Heatmaps show relative growth (% AUC_lin) following MBT and MHBT exposure with trace mineral supplementation (20 and 30 mL/L). Rows represent compound concentrations (1 ng/L–10 mg/L) and controls are included for comparison.Values are normalized to the solvent control (DMSO = 100%), with values >100% indicating higher relative growth in comparison to solvent control. Mineral supplementation largely restored growth of *C. aerofaciens*, except at the highest MBT concentration. Antibiotic (Clindamycin) control and blank control were also included for reliability and comparability of the assay.

Extended Growth Analysis Reveals Recovery of *C. aerofaciens* Following Benzothiazole Exposure

Additionally, growth curves revealed that *C. aerofaciens* exhibited slower growth compared to the majority of other gut strains following the 24 h assay, where only the lag phase and a portion exponential phase were captured. Therefore, a prolonged exposure experiment (~72 h) was conducted to capture the complete growth profile.

Despite an initial delay in growth being observed (Figure 11A; Figure 12A) in extended incubation time ~72 h (Figure 14) cultures recovered over extended incubation (~72 h; Figure 14). No significant reduction in total AUC was detected for *C. aerofaciens* following MBT or MHBT exposure compared with the solvent control (adjusted $p > 0.05$). These findings indicate that MBT caused a significant but transient early inhibitory effect at selected concentrations, whereas MHBT showed non-significant early inhibitory trends, despite a consistent inhibitory effect being observed within individual biological replicates.

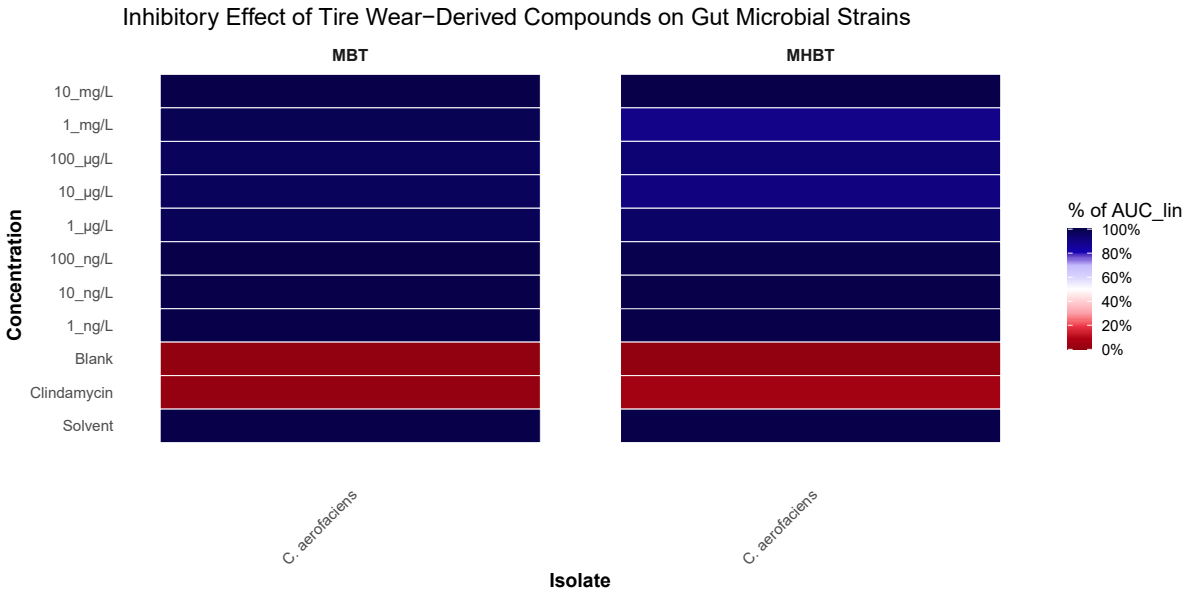

Figure 14: Prolonged inhibition of *C. aerofaciens* following benzothiazole treatment. As not all growth phases were captured during the standardized 24 h assay, *C. aerofaciens* was incubated with benzothiazoles for ~72 h to enable full characterization of its growth dynamics, including the stationary phase. Heatmaps display relative growth (% AUC_lin) after MBT and MHBT exposure during extended incubation (~72 h), until the stationary phase was reached. Growth values were normalized to the solvent control (DMSO = 100%), and antibiotic (Clindamycin) and blank control were included for comparison. No biologically relevant inhibition was observed across three biological replicates. Color intensity reflects the degree of growth inhibition, where dark blue indicates high growth (80% or greater), corresponding to no relevant inhibition (less than 20% of inhibition), whereas values below 80% growth (purple to red) indicate increasing levels of growth inhibition. No statistically significant growth reduction was observed after 72 h incubation with MBT or MHBT (adjusted $p > 0.05$).

Discussion

This study represents an initial effort to investigate the impact of selected organic tire wear particles (TWPs)-derived compounds, namely benzothiazoles (MBT and MHBT) and DPG, on human gut microbiota, using representative pure culture strains and high-throughput growth inhibition assays. While previous research has established the presence and biological activity of TWPs in environmental contexts, their effects, particularly on gut-resident bacteria, remain poorly understood despite established exposure routes for the human gut. Our findings indicate that despite overall resistance to exposure demonstrated by the majority of strains (no significant growth impacts across any tested concentration in nine out of ten strains tested), certain bacterial taxa are selectively susceptible to specific TWPs constituents including benzothiazoles, and that growth inhibition patterns can vary by compound, concentration, and microbial strain.

Despite this overall tolerance, strain-specific responses were observed. Most notably, *Collinsella aerofaciens* exhibited a delay in the onset of exponential growth following exposure to MBT and MHBT within each biological replicate. To a lesser extent, *Enterocloster bolteae* and *Akkermansia muciniphila* showed approximately 30 and 25% of inhibition at the highest tested concentration (10 mg/L), respectively, while *Lactobacillus hominis* was inhibited to a lesser extent, showing less than 20% growth inhibition at 10 mg/L concentration. Statistical comparisons versus solvent control showed that *C. aerofaciens* was the most responsive strain, exhibiting significant growth reduction after MBT treatment at 10 mg/L and 1 mg/L ($p = 0.0037$ and 0.041, respectively), while 100 µg/L narrowly missed the significance threshold ($p = 0.0505$). No other treatment concentration remained significant across the multi-strain screening dataset, although consistent and comparable effects were observed within individual biological replicates. However, it is important to note that these concentrations greatly exceed environmentally reported levels which range from ng/L to µg/L (Johannessen C. H., 2022; Johannessen C. S., 2022; Li Z. M., 2023; Li Z. M., 2023; Marques dos Santos, 2023). The remaining Gram-negative strains (*Alistipes putredinis*, *Bacteroides caccae*, *Bacteroides xylanisolvens*, *Bacteroides fragilis*, and *Escherichia coli*), as well as the Gram-positive *Enterococcus faecium* demonstrated complete tolerance at all screening concentrations. This pattern is consistent with previous findings that environmental pollutants often exert strain-specific effects, with marked differences in susceptibility among gut bacteria such as highly susceptible *Parabacteroides distasonis* versus more tolerant *Escherichia coli* and *Akkermansia muciniphila* (Roux I., 2025). In contrast, xenobiotic compounds such as pharmaceuticals are often associated with broad-spectrum toxicity (Maier, 2018).

The observed differences in susceptibility may be partially explained by bacterial cell envelope structure and defense mechanisms. Gram-positive bacteria have a single membrane and thick peptidoglycan wall, whereas Gram-negatives possess an inner membrane, a thin peptidoglycan layer, and an outer membrane (OM) enriched in negatively charged lipopolysaccharides (Smith, 2024). Hydrophilic molecules enter Gram-negative bacteria through porins, whereas hydrophobic xenobiotics penetrate primarily by diffusion through lipid regions of the outer membrane/LPS layer or after membrane disruption (Saxena, 2023). Upon entering Gram-negative bacteria, xenobiotics distribute across the periplasm, inner membrane (IM), and cytoplasm, sometimes binding locally (Masi, 2017). For hydrophobic agents such as benzothiazoles, the inner membrane is not a major barrier, however many strains

as *E. coli* possess active efflux pumps (e.g., AcrAB–TolC) which expel lipophilic compounds (Elkins, 2002; Ghotaslou, 2018). These features likely explain Gram-negative tolerance, though the resistance of *E. faecium* likely indicates additional defensive mechanisms such as AsrR mediated oxidative stress response (Lebreton, 2012). Further, recent work by Lindell et al. (2025) demonstrates that gut bacteria can actively bioaccumulate xenobiotics, with 38 strains accumulating per- and polyfluoroalkyl substances (PFAS) across nanomolar to 500 μM exposure ranges, and notably *Bacteroides uniformis* reaches millimolar intracellular concentrations, exceeding that of even some native metabolites, without impaired growth. Additionally, they demonstrated that in *Escherichia coli*, bioaccumulation increased in the absence of the TolC efflux pump, indicating that active efflux systems limit intracellular accumulation despite compound uptake (Lindell A. E.-C.-P., 2025). Further, a recent study demonstrated that PFAS, namely n:3 fluorotelomer carboxylates (FTCAs), can be covalently incorporated into bacterial lipid bilayer components (phosphatidylethanolamine and phosphatidylglycerol) of *Pseudomonas sp.* strain 273, *E. coli* and *Enterococcus faecalis* (Xie, 2026), providing direct evidence of chemical integration of xenobiotics into core cellular structures, rather than passive accumulation alone. This highlights that microbial tolerance to environmental compounds inferred by growth dynamics alone may not reflect a lack of microbe-xenobiotic interaction, but rather a balance between uptake, intracellular sequestration, and efflux processes that ultimately influence compound bioavailability, toxicity, and host exposure.

Mechanistically, benzothiazoles are aromatic heterocycles and largely hydrophobic (Tkalec, 2023). MBT has previously been reported to disrupt membrane permeability in anaerobic bacteria, specifically *E. coli*, at 100 mg/L (De Wever H. V., 1997; De Wever H. D., 1994), and demonstrates toxicity towards *Pseudomonas fluorescens*, *Paracoccus denitrificans*, and yeast at ~100 mg/L. Although the mechanism has yet to be fully investigated, potassium leakage has been observed in *E. coli* suggesting MBT may compromise membrane integrity and proton gradients (De Wever H. V., 1997). Further, the protective properties of MBT and MHBT arise from strong copper (Cu) chelation, which forms a stable protective surface layer and limits oxidation (Vernack, 2020) hence their extensive use as anti-corrosion agents (Tkalec, 2023). In addition, MBT also chelates lead (Pb), zinc (Zn), and magnesium (Mg) (Marabini, 2008; Hu, 2021). As Cu, Zn, and Mg are essential cofactors in enzymes (such as polyphenol oxidases, metalloproteases, and RNA polymerase) (Hsieh, 2023; Wehrl, 2000; Bag, 2017) chelation may thus impair enzyme activity and contribute to growth inhibition (Vernack, 2020; Tkalec, 2023). In this study, the rescue of the initial growth delay was shown with supplementation of trace minerals, supporting the hypothesis that benzothiazole-induced effects are, at least partially, mediated through metal chelation.

In addition, the increased sensitivity of *C. aerofaciens* may be linked to its physiological characteristics. As a catalase- and oxidase-negative bacterium (Kageyama, 1999; Bilen, 2016), this may lead to an increased vulnerability to oxidative stress in comparison to, catalase-positive *E. coli* for example (Hassan, 1978). Benzothiazoles (such as MBT) have been confirmed to induce reactive oxygen species (ROS)-mediated DNA damage and cytotoxicity in mammalian and fish cells, respectively (Qi, 2022; Zeng, 2016). The lack of catalase in *C. aerofaciens* may explain the observed higher sensitivity and observed delay in exponential phase onset. By contrast, *L. hominis*, though catalase-negative, encodes for example thioredoxin-based repair systems (Serrano, 2007), which may account for the comparative higher tolerance of this strain. The strong ROS-generating potential of MBT and MHBT therefore may go some way to explain the observed sensitivity of *C. aerofaciens* at ng/L

concentrations, while alternative defenses in *L. hominis* and *E. faecium* may confer protection resulting in exposure tolerance.

Importantly however, the inhibitory effect observed in *C. aerofaciens* was transient. Following prolonged incubation (~72 h), cultures recovered fully, despite the sustained presence of the pre-observed extended lag phase, and no biologically relevant long-term growth suppression was detected. This suggests that benzothiazole exposure primarily affects early growth dynamics rather than overall viability, likely reflecting temporary physiological stress as opposed to sustained toxicity. Although acute toxicity appeared limited, even transient growth delays may have ecological consequences, especially given the central role of *C. aerofaciens* in gut homeostasis. *C. aerofaciens* is one of the most abundant Actinobacteria in the healthy human gut, playing a key role in fermentation of complex carbohydrates into SCFAs, contribution to bile acid transformation, and supportive roles in vitamin B_{12} synthesis (Balabanova, 2021; Nguyen, 2025), with changes in its abundance being implicated in important adverse health consequences. It is also associated with IBD, Crohn's disease, psoriasis, atherosclerosis, non-alcoholic steatohepatitis (NASH), COVID-19, and responses to PD-1/PD-L1 immunotherapy (Nguyen, 2025; Kwon, 2023). Given its central role in gut homeostasis, the inhibition of *C. aerofaciens* by MBT and MHBT even in initial growth is notable and warrants further investigation.

Nonetheless, it is demonstrated that xenobiotic exposure can alter microbial metabolic activity independently of changes in community composition (Castañeda-Monsalve, 2024) with functional outputs, such as short-chain fatty acid (SCFA) production, being affected. Notably, benzotriazole exposure was associated with increased concentrations of major SCFAs – acetate, butyrate, and propionate (Castañeda-Monsalve, 2024). Furthermore, a recent study demonstrated that prolonged exposure to environmental pollution can promote the selection and proliferation of bacterial taxa in gut associated with the degradation of organic pollutants, many of which are also known for their roles in soil bioremediation (De Filippis, 2024). Together, these findings along with previous studies (Lindell A. E.-C.-P., 2025) highlight that even in the absence of detectable growth inhibition, xenobiotic exposure may still exert significant functional and ecological effects on the gut microbiome, potentially influencing host health outcomes.

Overall, the findings of this study indicate that representative human gut bacterial strains exhibit substantial tolerance to the tested tire wear particle–derived compounds, including benzothiazoles and DPG, notably at environmentally relevant concentrations, as well as elevated concentrations. While strain-specific responses were observed, most notably the delayed growth initiation of *Collinsella aerofaciens* treated with MBT, this effect was transient. The growth delay was alleviated by supplementation with trace minerals and cultures fully recovered during prolonged incubation, suggesting that the observed inhibition was reversible and likely associated with temporary physiological stress rather than sustained toxicity. These findings are consistent with recent work by Roux et al. (2025), who reported that the majority (over 900/1076) of environmental pollutants screened against 22 gut bacterial strains showed limited inhibitory activities and that inhibitory effects were often strain-specific as opposed to broadly toxic. Together, these results highlight the overall resilience of the majority of tested representative human gut bacteria to selected organic environmental contaminants under the tested conditions.

Conclusion

This study provides an initial assessment of the effects of selected tire wear particles (TWPs)-derived organic compounds on representative human gut bacterial strains. Overall, the tested strains exibited substantial tolerance to acute benzothiazole and DPG exposure, even at concentrations substantially exceeding those typically reported in the environment. These finding are encouraging, particularly due to the detection of benzothiazoles and DPG in the ng/L to low µg/L range and µg/L range, respectively in aquatic environments (Zhang H. Y., 2023), whereas sustained biologically relevant inhibition was not observed in this study even at much higher concentrations. In addition, *C. aerofaciens* recovered after prolonged incubation (~72 h), suggesting that the observed effect was transient and primarily affected early growth kinetics rather than long-term viability.

However, although only acute toxicity was observed, temporary growth delays may still have ecological implications. In the complex gut environment, where microbial competition and nutrient limitation shape microbial community dynamics (Reese, 2018), such delays in growth initiation of affected commensal bacteria could influence niche occupation and competitive interactions. Importantly, the absence of biologically significant growth inhibition does not preclude the occurrence of metabolic or functional alterations following exposure to benzothiazoles and phenyldiamines. Indeed, xenobiotic exposure has been shown to induce metabolic changes even in the absence of shifts in community composition (Castañeda-Monsalve, 2024). Furthermore, while *C. aerofaciens* demonstrated the ability to resume growth, suggesting adaptive or compensatory mechanisms that mitigate early stress responses under the tested conditions, these transient kinetic shifts may still carry ecological significance.

Taken together, these findings suggest that direct growth suppression of individual tested gut bacterial strains by environmentally relevant concentrations of benzothiazoles and DPG is likely limited under the conditions tested, suggesting neglible toxicity of the compounds themselves to the strains examined. Nevertheless, more subtle effects during chronic exposure cannot be excluded, including potential changes in microbial community composition, gene expression, metabolism, or interspecies interactions that may not be captured in single-strain growth assays. Therefore, future studies integrating community-level models and long-term exposure scenarios are essential to fully understand the potential impact of TWPs-derived compounds on gut microbiome function and host health. Further, investigating the cumulative and potentially synergistic effects of multiple TWPs-derived compounds is of critical importance, as real-world exposure occurs as complex mixtures rather than individual substances. This is especially relevant given that multiple classes of TWPs-associated compounds, including benzothiazoles and phenyldiamines, have been detected in commonly consumed leafy vegetables (Castan, et al., 2022; Sherman, 2024), suggesting that combined exposure may influence both individual strains and microbial community dynamics in ways not captured by single-compound studies. Overall, this study highlights that while acute toxicity of TWPs-derived compounds to individual gut bacterial strains appears limited at environmentaly relevant concentration, their potential to induce subtle yet ecologically relevant changes in microbial dynamics and function cannot be excluded and thus warrants further investigation.

Disclaimer

ChatGPT (OpenAI) and JenniAI were used as a language assistance tool to improve grammar and clarity of the manuscript. Additionally is used for primary literature search and to assist with Python and R scripting for data processing and visualization. The Abstract was translated into german using DeepL. All scientific ideas, data processing, data interpretation, and conclusions were developed independently by the author.

Bibliography

Sherman, A. L. (2024). Uptake of tire-derived compounds in leafy vegetables and implications for human dietary exposure. *Frontiers in Environmental Science*, 12, 1384506.

Sekirov, I. R. (2010). Gut microbiota in health and disease. *Physiological reviews.*

Santoro, A. O. (2018). Gut microbiota changes in the extreme decades of human life: a focus on centenarians. *Cellular and Molecular Life Sciences*, Cellular and Molecular Life Sciences, .

Jovel, J. D. (2018). The human gut microbiome in health and disease. *Metagenomics*, 197-213.

Gomaa, E. Z. (2020). Human gut microbiota/microbiome in health and diseases: a review. *Antonie Van Leeuwenhoek*, 113(12), 2019-2040.

Lozupone, C. A. (2012). Diversity, stability and resilience of the human gut microbiota. *Nature*, 489(7415), 220-230.

Trosvik, P. &. (2015). Ecology of bacteria in the human gastrointestinal tract—identification of keystone and foundation taxa. *Microbiome*, 3(1), 44.

Tudela, H. C. (2021). Next generation microbiome research: identification of keystone species in the metabolic regulation of host-gut microbiota interplay. *Frontiers in cell and developmental biology*, 9, 719072.

Štefanac, T. G. (2021). Xenobiotics—division and methods of detection: a review. *Journal of xenobiotics*, 11(4), 130-141.

Croom, E. (2012). Metabolism of xenobiotics of human environments. *Progress in molecular biology and translational science*, 112, 31-88.

Chi, L. T. (2021). Studies of xenobiotic-induced gut microbiota dysbiosis: from correlation to mechanisms. *Gut Microbes*, 13(1), 1921912.

Bidell, M. R. (2022). Gut microbiome health and dysbiosis: A clinical primer. *The Journal of Human Pharmacology and Drug Therapy*, 42(11), 849-857.

Perez, N. B. (2020). Dysbiosis of the gut microbiome: a concept analysis. *Journal of Holistic Nursing*, 38(2), 223-232.

Das, B. &. (2019). Homeostasis and dysbiosis of the gut microbiome in health and disease. *Journal of biosciences*, 44, 1-8.

Carding, S. V. (2015). Dysbiosis of the gut microbiota in disease. *Microbial ecology in health and disease*, 26(1), 26191.

Jin, Y. W. (2017). Effects of environmental pollutants on gut microbiota. *Environmental Pollution*, 222, 1-9.

Lefever, D. E. (2016). TCDD modulation of gut microbiome correlated with liver and immune toxicity in streptozotocin (STZ)-induced hyperglycemic mice. *Toxicology and applied pharmacology*, 304, 48-58.

Castañeda-Monsalve, V. F.-K. (2024). High-throughput screening of the effects of 90 xenobiotics on the simplified human gut microbiota model (SIHUMIx): a metaproteomic. *Frontiers in Microbiology*, 15, 1349367.

Johannessen, C. L. (2022). Composition and transformation chemistry of tire-wear derived organic chemicals and implications for air pollution. *Atmospheric Pollution Research*, 13(9), 101533.

Sommer, F. D. (2018). Tire abrasion as a major source of microplastics in the environment. *Aerosol and air quality research*, 18(8), 2014-2028.

Tumwet, F. C. (2025). Characterisation of tire wear particles and their chemical markers: A case study along a German highway. *Case Studies in Chemical and Environmental Engineering*, 11, 101163.

Alotaibi, M. D. (2015). Benzotriazoles in the aquatic environment: a review of their occurrence, toxicity, degradation and analysis. *Water, Air, & Soil Pollution*, 226(7), 226.

Tkalec, Ž. R. (2023). Contaminants of emerging concern in urine: a review of analytical methods for determining diisocyanates, benzotriazoles, benzothiazoles, 4-methylbenzylidene camphor, isothiazolinones, fragrances, and non-phthalate plasticizers. *Environmental Science and Pollution Research*, 30(42), 95106-95138.

Mathissen, M. S. (2011). Investigation on the potential generation of ultrafine particles from the tire–road interface. *Atmospheric Environment*, 45(34), 6172-6179.

Kundel, D. W. (2025). Tracks of travel: unveiling tire particle concentrations in Swiss cantonal road soils. *Microplastics and Nanoplastics*, 5(1), 6.

Baensch-Baltruschat, B. K. (2021). Tyre and road wear particles-A calculation of generation, transport and release to water and soil with special regard to German roads. *Science of the Total Environment*, 752, 141939.

Johannessen, C. H. (2022). The tire wear compounds 6PPD-quinone and 1, 3-diphenylguanidine in an urban watershed. *Archives of environmental contamination and toxicology*, 82(2), 171-179.

Tian, Z. Z. (2021). A ubiquitous tire rubber–derived chemical induces acute mortality in coho salmon. *Science*, 371(6525), 185-189.

Song, Q. M. (2025). Size-and duration-dependent toxicity of heavy vehicle tire wear particles in zebrafish. *Journal of Hazardous Materials*, 493, 138299.

Liu, J. Y. (2024). Comparative toxic effect of tire wear particle-derived compounds 6PPD and 6PPD-quinone to Chlorella vulgaris. *Science of the Total Environment*, 951, 175592.

Ding, J. Z. (2020). Dysbiosis in the gut microbiota of soil fauna explains the toxicity of tire tread particles. *Environmental Science & Technology*, 54(12), 7450-7460.

Peng, C. (2024). Adverse effect of TWPs on soil fungi and the contribution of benzothiazole rubber additives. *Journal of Hazardous Materials*, 479: 135574.

Yekeler, H. &. (2006). Predicting the efficiencies of 2-mercaptobenzothiazole collectors used as chelating agents in flotation processes: a density-functional study. *Journal of molecular modeling*, 12(6), 763-768.

Liao, C. K. (2018). A review of environmental occurrence, fate, exposure, and toxicity of benzothiazoles. *Environmental science & technology*, 52(9), 5007-5026.

Li, Z. M. (2023). Occurrence of 1, 3-diphenylguanidine, 1, 3-di-o-tolylguanidine, and 1, 2, 3-triphenylguanidine in indoor dust from 11 countries: implications for human exposure. *Environmental Science & Technology*, 57(15), 6129-6138.

Johannessen, C. S. (2022). Air monitoring of tire-derived chemicals in global megacities using passive samplers. *Environmental Pollution*, 314, 120206.

Li, Z. M. (2023). 1, 3-Diphenylguanidine, benzothiazole, benzotriazole, and their derivatives in soils collected from northeastern United States. *Science of The Total Environment,* , 887, 164110.

Marques dos Santos, M. &. (2023). Occurrence of polymer additives 1, 3-diphenylguanidine (DPG), N-(1, 3-dimethylbutyl)-N′-phenyl-1, 4-benzenediamine (6PPD), and chlorinated byproducts in drinking water: contribution from plumbing polymer materials. *Environmental Science & Technology Letters*, 10(10), 885-890.

Shin, H. M. (2020). Measured concentrations of consumer product chemicals in California house dust: implications for sources, exposure, and toxicity potential. *Indoor Air*, 30(1), 60-75.

Jin, Y. C. (2023). Recent review on selected xenobiotics and their impacts on gut microbiome and metabolome. *TrAC Trends in Analytical Chemistry*, 166, 117155.

Zhu, B. W. (2010). Human gut microbiome: the second genome of human body. *Protein & cell*, 1(8), 718-725.

Shin, J. H. (2024). Bacteroides and related species: The keystone taxa of the human gut microbiota. *Anaerobe*, 85, 102819.

Rieger, P. G. (2002). Xenobiotics in the environment: present and future strategies to obviate the problem of biological persistence. *Journal of Biotechnology*, 94(1), 101-123.
Tsiaoussis, J. A. (2019). Effects of single and combined toxic exposures on the gut microbiome: Current knowledge and future directions. *Toxicology letters*, 31.
Wik A., D. G. (2009). Occurrence and effects of tire wear particles in the environment – A critical review and an initial risk assessment. *Environmental pollution,*, 157(1), 1-11.
Roux I., L. E. (2025). Industrial and agricultural chemicals exhibit antimicrobial activity against human gut bacteria in vitro. *Nature Microbiology*, 1-15.
Ghanadi M., C. L. (2025). Tire-wear particles and tire-related emerging contaminants: Characteristics, occurrence, and toxicity in the environment. *Current Opinion in Environmental Science & Health*, Volume 48, 100666.
Lindell, A. E.-K. (2022). Multimodal interactions of drugs, natural compounds and pollutants with the gut microbiota. *Nature Reviews Microbiology*, 20(7), 431-443.
Nakov, R. &. (2020). Chemical metabolism of xenobiotics by gut microbiota. *Current Drug Metabolism*, 21(4), 260-269.
Zhang, S. J. (2015). Subchronic exposure of mice to cadmium perturbs their hepatic energy metabolism and gut microbiome. *Chemical research in toxicology*, 28(10), 2000-2009.
Lu, K. A. (2014). Arsenic exposure perturbs the gut microbiome and its metabolic profile in mice: an integrated metagenomics and metabolomics analysis. *Environmental health perspectives*, 122(3), 284.
Lukovac, S. B. (2014). Differential modulation by Akkermansia muciniphila and Faecalibacterium prausnitzii of host peripheral lipid metabolism and histone acetylation in mouse gut organoids. *MBio*, 5(4), 10-1128.
Zhang, L. N. (2015). Persistent organic pollutants modify gut microbiota–host metabolic homeostasis in mice through aryl hydrocarbon receptor activation. *Environmental health perspectives*, 123(7), 679.
Van de Wiele, T. V. (2005). Human colon microbiota transform polycyclic aromatic hydrocarbons to estrogenic metabolites. *Environmental health perspectives*, 113(1), 6-10.
Boratyn, G. M. (2013). BLAST: a more efficient report with usability improvements. *Nucleic acids research*, 41(W1), W29-W33.
Davis, M. W. (2022). ApE, a plasmid editor: a freely available DNA manipulation and visualization program. *Frontiers in bioinformatics*, 2, 818619.
Midani, F. S. (2021). AMiGA: software for automated analysis of microbial growth assays. *Msystems*, 6(4), 10-1128.
Wickham, H. (2011). ggplot2. *Wiley interdisciplinary reviews: computational statistics*, 3(2), 180-185.
Korth, N. Y.-M. (2024). Genomic co-localization of variation affecting agronomic and human gut microbiome traits in a meta-analysis of diverse sorghum. *G3: Genes, Genomes, Genetics*, 14(9), jkae145.
Kijner, S. E. (2024). CRISPR-Cas-based identification of a sialylated human milk oligosaccharides utilization cluster in the infant gut commensal Bacteroides dorei. *Nature communications*, 15(1), 105.
Zhou, H. Z. (2024). A citric acid cycle-deficient Escherichia coli as an efficient chassis for aerobic fermentations. *Nature communications*, 15(1), 2372.
Nyberg, S. D. (2007). Long-term antimicrobial resistance in Escherichia coli from human intestinal microbiota after administration of clindamycin. *Scandinavian journal of infectious diseases*, 39(6-7), 514-520.
Maier, L. P. (2018). Extensive impact of non-antibiotic drugs on human gut bacteria. *Nature*, 555(7698), 623-628.

Smith, B. L. (2024). Escherichia coli resistance mechanism AcrAB-TolC efflux pump interactions with commonly used antibiotics: a molecular dynamics study. *Scientific Reports*, 14(1), 2742.
Masi, M. R. (2017). Mechanisms of envelope permeability and antibiotic influx and efflux in Gram-negative bacteria. *Nature microbiology*, 2(3), 1-7.
Elkins, C. A. (2002). Substrate specificity of the RND-type multidrug efflux pumps AcrB and AcrD of Escherichia coli is determined predominately by two large periplasmic loops. *Journal of bacteriology*, 184(23), 6490-6498.
Ghotaslou, R. Y. (2018). The role of efflux pumps in Bacteroides fragilis resistance to antibiotics. *Microbiological research*, 210, 1-5.
Lebreton, F. V.-C. (2012). AsrR is an oxidative stress sensing regulator modulating Enterococcus faecium opportunistic traits, antimicrobial resistance, and pathogenicity. *PLOS Pathogens*.
Lindell, A. E.-C.-P. (2025). Human gut bacteria bioaccumulate per-and polyfluoroalkyl substances. *Nature Microbiology*, 10(7), 1630-1647.
De Wever, H. V. (1997). Inhibitory effects of 2-mercaptobenzothiazole on microbial growth in a variety of trophic conditions. *Environmental toxicology and chemistry*, 16(5), 843-848.
Vernack, E. C. (2020). DFT studies of 2-mercaptobenzothiazole and 2-mercaptobenzimidazole as corrosion inhibitors for copper. *Corrosion Science*, 174, 108840.
Marabini, A. M. (2008). Thermodynamic approach for the evaluation of the reactivity of mercaptobenzothiazole reagents with Pb and Zn cations; correlation with results of flotation. *Mineral Processing and Extractive Metallurgy*, 117(1), 43-47.
Hu, T. O. (2021). One-pot scalable in situ growth of highly corrosion-resistant MgAl-LDH/MBT composite coating on magnesium alloy under mild conditions. *Journal of Materials Science & Technology*, 92, 225-235.
Hsieh, M. L. (2023). Biochemistry, RNA polymerase. *StatPearls Publishing*.
Wehrl, W. N. (2000). The FtsH protein accumulates at the septum of Bacillus subtilis during cell division and sporulation. *Journal of bacteriology*, 182(13), 3870-3873.
Bag, S. G. (2017). Complete genome sequence of Collinsella aerofaciens isolated from the gut of a healthy Indian subject. *Genome Announc 5*, e01361-17.
Kageyama, A. B. (1999). Phylogenetic and phenotypic evidence for the transfer of Eubacterium aerofaciens to the genus Collinsella as Collinsella aerofaciens gen. nov., comb. nov. *International Journal of Systematic and Evolutionary Microbiology*, 49(2), 557-565.
Bilen, M. C. (2016). "Collinsella bouchesdurhonensis" sp. nov., identified in human stool sample. *New Microbes and New Infections*, 17, 39.
Hassan, H. M. (1978). Regulation of the synthesis of catalase and peroxidase in Escherichia coli. *Journal of Biological Chemistry*, 253(18), 6445-6450.
Qi, Y. T. (2022). 2-mercaptobenzothiazole generates γ-H2AX via CYP2E1-dependent production of reactive oxygen species in urothelial cells. *Journal of Biochemical and Molecular Toxicology*, 36(6), e23043.
Zeng, F. S. (2016). Evaluating the toxic potential of benzothiazoles with the rainbow trout cell lines, RTgill-W1 and RTL-W1. *Chemosphere*, 155, 308-318.
Serrano, L. M. (2007). Thioredoxin reductase is a key factor in the oxidative stress response of Lactobacillus plantarum WCFS1. *Microbial Cell Factories*, 6(1), 29.
Nguyen, V. K. (2025). Collinsella and Prevotella: Mixed Systemic Actions of a Dynamic Duo. *Clinical Infection & Immunity*.

Balabanova, L. A. (2021). Microbial and genetic resources for cobalamin (vitamin B12) biosynthesis: From ecosystems to industrial biotechnology. *International Journal of Molecular Sciences*, 22(9), 4522.

Kwon, J. B. (2023). Collinsella aerofaciens produces a pH-responsive lipid immunogen. *Journal of the American Chemical Society*, 145(13), 7071-7074.

De Filippis, F. V. (2024). Exposure to environmental pollutants selects for xenobiotic-degrading functions in the human gut microbiome. *Nature Communications*, 15(1).

Zhang, H. Y. (2023). Occurrence and risks of 23 tire additives and their transformation products in an urban water system. *Environment International*, 171, 107715.

Reese, A. T. (2018). Microbial nitrogen limitation in the mammalian large intestine. *Nature microbiology*, 3(12), 1441-1450.

De Wever, H. D. (1994). Toxicity of 2-mercaptobenzothiazole towards bacterial growth and respiration. *Applied microbiology and biotechnology*, 42(4), 631-635.

Liu, J. F. (2023). Acute toxicity of tire wear particles and leachate to Daphnia magna. *Comparative Biochemistry and Physiology Part C: Toxicology & Pharmacology*, 272, 109713.

Müller, A. K. (2022). Determination of tire wear markers in soil samples and their distribution in a roadside soil. *Chemosphere*, 294, 133653.

Jeong, S. H. (2025). The Influence of polycyclic aromatic hydrocarbons exposure on the gut microbiome composition and inflammatory responses. *Ecotoxicology and environmental safety*, 303, 118910.

Wagner S., H. T. (2018). Tire wear particles in the aquatic environment - A review on generation, analysis, occurrence, fate and effects. *Water research*, 139, 83-100.

Xie, Y. C. (2026). Bacteria covalently incorporate polyfluoroalkyl carboxylates into membrane lipids. *Nature Microbiology*, 1-11.

Trabalón, L. M. (2017). Determination of benzothiazoles in seafood species by subcritical water extraction followed by solid-phase microextraction-gas chromatography-tandem mass spectrometry: estimating the dietary intake. *Analytical and bioanalytical chemistry*, 409(23), 5513-5522.

Wu, X. L. (2025). Exposure to environmental xenobiotics and lung tissue function: A comprehensive review on biological mechanisms and pathways. *Ecotoxicology and Environmental Safety*, 308, 119438.

Zeb, A. R. (2026). A critical review of tire wear particles aging and ecotoxicological consequences in terrestrial environments: Insights into environmentally persistent free radicals. *Journal of Hazardous Materials*, 140641.

Castan, S., Sherman, A., Peng, R., Zumstein, M. T., Wanek, W., Hüffer, T., & and Hofmann, T. (2022). Uptake, metabolism, and accumulation of tire wear particle-derived compounds in lettuce. *Environmental science & technology*, 57(1), 168-178.

Saxena, D. R. (2023). ackling the outer membrane: facilitating compound entry into Gram-negative bacterial pathogens. *npj Antimicrobials and Resistance*, 1(1), 17.

Banerji, S. B. (1982). Metal complexes of 2-mercaptobenzothiazole. *Transition metal chemistry*, 7(1), 5-10.

Wickham, H. M. (2019). Welcome to the Tidyverse. *Journal of open source software 4, no. 43 (2019): 1686.*, 4, no. 43: 1686.

Karyab, H. Y. (2016). Carcinogen risk assessment of polycyclic aromatic hydrocarbons in drinking water, using probabilistic approaches. *Iranian journal of public health*, 45(11), 1455.

Benjamini, Y. a. (1995). Controlling the false discovery rate: a practical and powerful approach to multiple testing. *Journal of the Royal statistical society: series B (Methodological)*, 57(1), 289-300.

Welch, B. L. (1947). The generalization of ‘STUDENT'S’problem when several different population varlances are involved. *Biometrika*, 34(1-2), 28-35.

Zusammenfassung

Reifenabriebpartikel sind eine weit verbreitete und zunehmend bedeutende Quelle für Umweltverschmutzung. Sie stellen ein komplexes Gemisch organischer Verbindungen dar, darunter Benzothiazole und Diphenylguanidin (DPG), die in verschiedenen Umweltbereichen sowie in Lebensmitteln immer häufiger nachgewiesen werden. Trotz wachsender Besorgnis hinsichtlich der Exposition des Menschen sind ihre Auswirkungen auf das Darmmikrobiom nach wie vor kaum erforscht. Ziel dieser Studie war es, mithilfe von Hochdurchsatz-Wachstumshemmungstests zu untersuchen, ob ausgewählte aus Reifen-stammende Verbindungen wie 2-Mercaptobenzothiazol (MBT), 5-Methyl-1H-benzotriazol (MHBT) und Diphenylguanidin (DPG) das Wachstum repräsentativer menschlicher Darmbakterienstämme beeinflussen. Insbesondere sollte im Rahmen dieser Arbeit ermittelt werden, ob diese Verbindungen die Wachstumsdynamik in Reinkulturen verändern, was auf das Potenzial für Verschiebungen in der mikrobiellen Zusammensetzung und damit letztlich auf eine Darmdysbiose hindeuten könnte, sowie die zugrunde liegenden Mechanismen der beobachteten Effekte untersucht werden.

Über einen weiten Konzentrationsbereich (ng/L bis mg/L) zeigten die meisten Stämme eine erhebliche Toleranz sowohl gegenüber Benzothiazolen als auch gegenüber DPG, wobei bei umweltrelevanten Konzentrationen oder darüber hinaus für die Mehrheit der Stämme keine biologisch relevante Wachstumshemmung beobachtet wurde. Es wurden jedoch stammspezifische Reaktionen festgestellt, wobei *Collinsella aerofaciens* nach Exposition gegenüber MBT und MHBT unabhängig von der Konzentration eine leichte konsistente Verzögerung beim Einsetzen des exponentiellen Wachstums zeigte. Dieser Effekt war vorübergehend. , *C. aerofaciens* Kulturen erholten sich bei längerer Inkubation vollständig, was auf einen Einfluss auf die frühe Wachstumskinetik aber nicht auf die langfristige Lebensfähigkeit hindeutet. Bemerkenswerterweise milderte die Zugabe von Spurenelementen die Wachstumsverzögerung, was darauf hindeutet, dass die metallchelierende Aktivität von Benzothiazolen zum zugrunde liegenden Mechanismus beitragen könnte.

Das Verständnis, wie die Exposition zentraler Stämme des Darmmikrobioms gegenüber diesen Xenobiotika ihr Wachstumsverhalten beeinflusst, liefert Einblicke in mögliche Störungen, die innerhalb des komplexen Darmökosystems auftreten können. Dieses Wissen ist unerlässlich für die Bewertung möglicher gesundheitlicher Folgen, die mit der Umweltexposition gegenüber Schadstoffen verbunden sind. Neue Erkenntnisse deuten darauf hin, dass Xenobiotika funktionelle Veränderungen, wie beispielsweise eine veränderte Produktion kurzkettiger Fettsäuren, unabhängig von Veränderungen der mikrobiellen Abundanz induzieren können. Daher sind, obwohl die direkte Wachstumshemmung durch Chemikalien aus Reifenabrieb minimal sein mag, potenzielle Auswirkungen auf die mikrobielle Funktion, die Interaktionen zwischen den Arten und die langfristige Dynamik der Gemeinschaft nicht auszuschließen. Dennoch zeigt diese Studie eine insgesamt erhebliche Toleranz ausgewählter Darmstämme gegenüber der Exposition gegenüber den untersuchten Verbindungen, sowie stammspezifische Auswirkungen auf die Wachstumsdynamik und liefert erste mechanistische Einblicke in die Wirkmechanismen dieser Verbindungen. Diese Arbeit schafft somit eine Grundlage für zukünftige Forschung, die auf komplexe mikrobielle Gemeinschaften angewendet werden könnte, um die Auswirkungen auf die Stabilität des Darmmikrobioms und die Gesundheit des Wirts besser zu verstehen.